

We thank reviewer#1 for his/her thorough and constructive review. Analytical replies to reviewer's comments are provided below. The reviewer's comments are in blue. Line numbers refer to the version with track changes.

The paper describes the UVC III campaign for calibrating and intercomparing solar UV radiometers, which was held in Davos, Switzerland, from June to August 2022, involving filter radiometers and the portable reference spectroradiometers QASUME and QASUMEII. However, the focus is on incremental improvements of the radiative transfer modeling tool (UVIOS2), which was used to forecast the UV index (UVI) with inputs from satellite, reanalysis, and ground-based sources.

Comparisons with the reference QASUME UVI measurements were used to demonstrate overall good performance of the model for clear skies, i.e., when the sun was not covered by clouds. However, much larger differences were found with instantaneous and daily UVI measurements, which were explained by cloud modeling challenges (Fig.5). Under cloud-free skies enhanced aerosol absorption, i.e., low single scattering albedo (SSA), might have explained model overestimation (Fig. 3 and 4), but there were no SSA measurements in UV to confirm this hypothesis.

#### Reply

In the revised version we used AERONET SSA (at 440 nm) data to extract safer conclusions and further support the discussion.

There is very brief mention of comparisons between QASUME and filter radiometers in section 3.3 and Figure 10 (previously published) shows that the results mainly depend on application of the consistent calibration factors (PMOD/WRC). This section needs to be either expanded or removed.

#### Reply

The UVC III campaign has been analytically described in the corresponding WMO report (Hülsen and Gröbner, 2023). This paper is mainly focused on exploiting the results of the campaign to quantify the accuracy of the UVIOS2 model. We agree that some information about the campaign should be provided for the readers' convenience, and we expanded section 3.3.

**UVI references are incomplete.**

#### Reply

More than 15 new references were added in the manuscript.

**The paper may be suitable for publication after improving quality of the figures and completeness of the text and addressing technical questions described below.**

## Reply

We did our best to improve all aspects described above.

### RT modeling approach.

More details are needed describing extraterrestrial solar irradiance source, e.g., spectral smoothing applied, comparison with the state-of-the-art satellite TSIS-1 hybrid solar reference spectrum [Coddington, et al., <https://doi.org/10.1029/2022EA002637> ].

Such information has been added in the manuscript. See the corresponding reply to the specific comments below.

The aerosols are included into the cloudless LUT (Tables 1, 2). This is different to OMI and TROPOMI satellite UVI retrievals, where aerosol and cloud effects are parameterized as a separate scattering (Cc) and absorbing (Ca) correction factors,  $UV = Ca(SZA, AAOD) * Cc(SZA, COT, ...) * UV_{clear}(SZA, TOC, ...)$  [Arola et al., 2021 <https://doi.org/10.5194/amt-14-4947-2021>]. This explicit absorbing aerosol correction based on aerosol absorption optical depth (AAOD) would be especially important for North Africa and Middle East sites affected by desert dust, e.g. Roshan et al., *Atmosphere* 2020, 11, 96; doi:10.3390/atmos11010096.

Using aerosol optical thickness in UV (e.g., 340nm or 380nm) would be more appropriate as inputs to UVIOS2 model, because extrapolating visible AE would result in systematic overestimation of AOD in UV, e.g., see Fig 1 in Eck, et al., "Wavelength dependence of the optical depth of biomass burning, urban and desert dust aerosols," *J. Geophys. Res.* 104, 31333–31350, 1999.

Using cloud optical thickness in UV would be more accurate, e.g., Krotkov, et al., "Satellite estimation of spectral surface UV irradiance 2. Effects of homogeneous clouds and snow", *J. Geophys. Res.*, <http://doi.wiley.com/10.1029/2000JD900721>

## Reply

A more accurate scheme for aerosols and clouds would increase the size of the LUT and the complexity of the simulations, and consequently the computational time which would not allow us to provide the UVI on near real time. Discussion relative to the uncertainties related to the parameterization of the spectral behavior of the absorbing aerosols, as well as with the use of the CMF instead of COT has been added in section 2.2 (lines 230 – 234, 245 - 247).

### Measurements:

High mountain site is not ideal for the absolute hemispherical irradiance measurements due to horizon obstruction by mountains. Provide mountain elevation

**at the measurements site as function of the azimuth (in Figure 1) and estimate horizon blockage correction, which needs to be applied to the model and/or measurements.**

**Reply**

See our reply later on, in the corresponding specific comment.

**Clarify the difference between “clear-sky” (i.e., sun not blocked by clouds [line 275]) and “cloudless” (i.e., “clear sky”, [line 180]) conditions. Provide separate comparisons statistics for completely cloud-free periods.**

**Reply**

The difference between the terms “clear-sky” and “cloudless-sky” has been clarified. A new figure (Figure 5 in the new version) has been added to further discuss the effects of clouds that do not cover the solar disc.

**Describe correction for a non-lambertian angular response of the QASUME and radiometers involved into the UVC III campaign.**

**Reply**

A detailed description of this correction has been already provided in Hulsen et al., 2016

**Technical comments:**

**Figure 1: It would be useful to add a panoramic photo of the site and angular horizon elevation table for the observation site at PMOD. Calculate the correction factor in UVIOS2 to account for the horizon blockage effect at different SZAs.**

**Reply**

We have quantified the error in the simulated UVI due to the limited horizon. Since the error is smaller than 2%, i.e., well below the overall uncertainty in our simulations, we decided not to include a correction in our model.

**Figures 2, 8-9: Add year in X-axis. Use logarithmic Y-scale. Symbols are difficult to see. Use different and larger symbols and line styles.**

**Reply**

Figures 1, 8 (now 9), and 9 (now 10) have been updated. Though, we did not use a logarithmic scale because we believe that it will make the interpretation of the results by the readers more difficult.

**55 future climatic changes – climate changes**

**Reply**

Done

**73-74. limited by the finite width of the satellite pixel – reword**

**Reply**

Done

**74 weakness of satellite sensors – need clarification**

**Reply**

We tried to clarify by adding more information after lines 73-74 (in the original version):

The accuracy of satellite-based estimates is limited due to the finite width of the satellite pixel (Kazadzis et al., 2009) and the weakness of satellite sensors to accurately probe the lower troposphere (Bais et al., 2019). In particular, assumptions are made in the satellite algorithms to describe the complex interactions between radiation, aerosols and clouds, which increase the uncertainty in the retrievals. Uncertainties in the assumed aerosol properties (Arola et al., 2021; Parisi et al., 2021), inaccurate distinction of the effect of highly reflecting terrains and cloudiness (e.g., Lakkala et al., 2020b), and uncertainties in the description of cloud cover over high-altitude sites (e.g., Schenzinger et al., 2023) are among the uncertainty sources.

**77-78: Copernicus Atmospheric Monitoring Service (CAMS) – Atmosphere**

**Reply**

Done

**100 information of the public – information to the public**

**Reply**

Done

**117 reconstructed UVI series - reconstruct**

**Reply**

Done

**118 The UVIOS (UV-Index Operating System) nowcasting system that its basic features have been already described ... - reword sentence**

**Reply**

Done

**126 summarized as follows – use colon :**

**Reply**

Done

**147 data were used as a reference****Reply**

Done

**168 serves as a reference****Reply**

Done

**197 atlas plus modtan extraterrestrial spectrum – What was spectral resolution of ETS? Was a spectral smoothing and Sun-Earth distance correction applied? Compare with the TSIS-1 HRRS [Coddington et al., <https://doi.org/10.1029/2022EA002637>]**

**Reply**

We thank the reviewer for pointing out the significant role of the used ETS in our results.

The spectral resolution of the used ETS is 0.05 nm, so there was no need for spectral smoothing (simulations were performed with a step of 0.5 nm). As already mentioned in the original version of the manuscript (line 317):

“The cloudless-sky UVI LUT outputs were in all cases post corrected for the effect of the varying Earth-Sun distance and for the surface elevation (1596 m for Davos).”

Regarding the use of Atlas-plus-modtran ETS, we have added the following lines in the manuscript (lines 214 - 217):

“Using a different ETS might result to differences in the simulated erythemal irradiances, as for example was shown in the study of Gröbner et al., (2017). Based on the results of the latter study we estimate that the simulated irradiances might differ by up to 5% if a different ETS was used, making the used ETS spectrum a major uncertainty factor in UVIOS2 simulations.“

As suggested by the reviewer, we calculated the ratio between the erythemal irradiance that was calculated using Atlas-plus-modtran, and the erythemal irradiance that was calculated using TSIS-1 HRRS (considering wavelengths longer than 298 nm). When the latter ETS was used, erythemal irradiance at TOA was ~ 3.5% lower, which is generally in agreement to what is written in the manuscript.

**201 The US standard atmosphere (Anderson et al., 1986) was used – This model was not developed for a mountainous Davos site.**

**Reply**

Indeed, the standard US atmosphere is not necessarily representative for mountainous sites such as Davos. Nevertheless, the UVIOS2 has been developed to operate for a much wider region which includes mainly lower altitude locations. In the revised version we also added the following discussion (line 439 - 443)

“Considering invariant atmospheric properties (i.e., pressure and temperature profiles) based on a standard atmospheric profile (Anderson et al., 1986) which is not necessarily representative for a mountainous site such as Davos, introduces additional uncertainty, which however is expected to be minor relative to the overall uncertainty budget in our estimates. The used ETS and ozone absorption cross sections are more significant uncertainty factors (see Section 2.2).”

**202 the surface albedo was set to 0.05 – this may not be representative for N. Africa or Middle East sites.**

**Reply**

Indeed, there is already some discussion about surface albedo in the original version of the manuscript. The following sentence has been added (line 227):

“Adjustment of the surface albedo to the local conditions when UVIOS is used over more reflective terrains (e.g., deserts, snow-covered surfaces) is within the model improvements that are planned for the future since under such conditions assuming a standard value of 0.05 could result in large uncertainties (e.g., Weihs et al., (2001)).”

**205 A correction for the effect of altitude, assuming an increase of 5% per km – There is a strong spectral dependence of the UV increase with altitude ~5% at 330nm to ~10% at 290nm, e.g., see Fig. 7 in Krotkov et al., JGR, <http://doi.wiley.com/10.1029/98JD00233>**

**Reply**

We agree with the reviewer. There was already discussion in the introduction about the effect of altitude. The proposed reference has been added in the introduction:

“In general, the change in the levels of the solar UV irradiance with altitude depends on atmospheric composition and has a strong wavelength dependence which is introducing difficulties in the modelling of the UVI at mountainous sites (e.g., (Dvorkin and Steinberger, 1999; Krotkov et al., 1998)). At very high-altitude (or/and latitude) sites, ice and/or snow may persist even in late spring and summer resulting in extremely high UV exposure (e.g., (Schmalwieser et al., 2017b; Siani et al., 2008; Utrillas et al., 2016)).”

Nevertheless, the uncertainties due to this assumption (of the 5% increase with altitude) were quantified by performing simulations for the altitude of Davos, and for 95% of the cases the agreement was better than 2%.

**230 Analyses of different AERONET datasets shows – show**

**Reply**

Done

**231 around a typical [value]**

**Reply**

Done

**232 Given that ASY generally increases? with wavelength - ASY should decrease with wavelength**

**Reply**

It was a typo. It has been corrected

**241-244 Table 2: If input parameters are the same (SSA, ASY, surface albedo) they do not need to be included in the table.**

**Reply**

The corresponding rows have been deleted.

**245: Re-word the sentence.**

**Reply**

Done

**267 Level 2 AERONET retrievals were not used because they are not available yet. – They are available with a longer latency and could be used for reanalysis.**

**Reply**

The manuscript has been modified according to the reviewer's suggestion.

**268 nearly real time - near real time**

**Reply**

Done

**275 For the analysis, measurements were classified as clear-sky (i.e., sun was not fully or partially covered by clouds) – This classification is not consistent with the “clear-**

**sky” assumption in UVIOS2 model, where “clear-sky” is defined as “cloudless” conditions (line 182). This leads to inconsistencies in “clear sky” model to measurement comparison results.**

**Reply**

The reviewer is right. The UVI has been simulated for cloudless skies (now defined as cloudless skies), while the comparison with ground based measurements has been performed for unoccluded solar disk (now defined as clear-sky). The manuscript has been revised so this is clear in the new version.

**287: Under clear-skies – This case includes scattered clouds not blocking the sun. It would be useful to show a separate comparison for the cloud-free periods in Fig 2.**

Done. Figure 5 has been added to the manuscript.

**287-288: Remove “both”**

**Reply**

Done

**Figure 2: Add Year in X-axis. Symbols are difficult to discriminate. Use different and larger symbols and different line styles. It would be useful to show cloud-free periods using different symbols.**

**Reply**

Larger symbols are used in Figures 2, 8, 9 (2,9,10 in the new version) in the revised version of the manuscript. Year has been added in X-axis. Cloud-free cases have been analyzed separately, and a new figure has been added (Figure 5 in the new version).

**Calculating average UVI ratio between DOY 190 and 200 would result in positive bias, while the bias is negative between DOY 200 and 210. Is there an explanation?**

**Reply**

The negative bias for DOY 200 – 210 is explained by the combination of the following causes:

- According to AERONET measurements much larger AOD values were recorded during DOY 200 – 210 with respect to DOY 190 – 200 (AOD at 340 nm of 0.6 or more in DOY 201-202). The SSA in these days was very high (0.98 – 0.99 at 440 nm). As can be perceived by Figure 4, the underestimation of the SSA for the modelling of the UVI was a significant factor resulting in the negative bias.
- Broken clouds (Fig. 5, 6) around the sun also resulted in enhanced real UVI, but their role was minor relative to that of the SSA.

It is also clear from Fig. 4 that for low AOD ( $<0.05$ ) conditions (as in DOY 190 - 200) the model overestimates the UVI (on average by  $\sim 3\%$ ) which can be due to the combined effect of uncertainties in ETS. This is possibly the reason for the (on average) positive bias during these days. Furthermore, on DOY197-199, when larger AOD values have been recorded, the SSA (AERONET level 1.5 SSA at 440 nm) was below 0.9, which again justifies part of the positive bias.

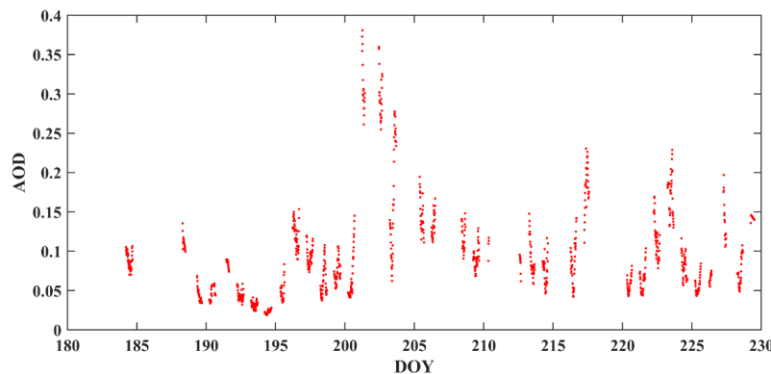


Figure: AOD at 500 nm from AERONET.

Part of the above discussion has been added to the revised version of the manuscript.

**295 Figure 2 shows that using highly accurate inputs for TOC, AOD at 500 nm, and AE does not result in a noticeable improvement in the accuracy of the modeled average clear-sky UVI. StDev decrease by less than 10% by using GB inputs**

#### Reply

The manuscript has been modified properly.

**302 Differences in AOD are in all cases within  $\pm 0.1$  - There are larger differences in Fig. A1**

#### Reply

Indeed, there are larger differences. The manuscript has been modified properly. The following lines have been added (line 356):

“When differences in AOD are larger (e.g., in DOY 201 – 202 the AOD from CAMS is lower by 0.15 – 0.25 relative to the AOD from CIMEL, i.e., CAMS has not captured the large AOD levels over the site) they result in correspondingly larger differences between the ratios (of 10 – 20%).”

**304-305 on average, TEMIS slightly underestimates TOC – TEMIS TOC is higher than Brewer TOC in Fig. A2**

**Reply**

Corrected

**309: differences in AOD – Use Brewer measured AOD.**

**Reply**

We decided to use AERONET data together with the AE provided by AERONET for various reasons. Main reasons:

- For Calibration and uncertainty issues as AERONET uses a globally standardized sun photometer network with rigorous automatic calibration procedures, ensuring high accuracy ( $\pm 0.01$  to  $\pm 0.02$  in AOD) while Brewer instruments rely on manual calibration. AOD below 320 nm from the Brewer, that would be more accurate for our work, is highly uncertain as discuss in the relevant bibliography.
- And mostly as AERONET spatial global coverage helps more for more “global” use of models like UVIOS2.

**Με σχόλια [if1]:** I am not sure what I should reply here.  
First of all, is the AOD from Brewer available?

**313: ranging from values smaller than 0.8 (during e.g., events of dust or biomass burning aerosols – These events are not typical for Davos location. Please, provide evidence if such events did occur during UVC-III campaign.**

**Reply**

We added some discussion in this section based on the SSA values measured at 440 nm by the CIMEL. The added discussion provides additional evidence for the role of SSA. Furthermore, we added “polluted aerosols” in the parenthesis, that were possibly transferred from Germany in these days. We could not find any evidence that the site was affected by dust or smoke aerosols.

**Figure 3. Why show a hypothetical case with SSA=0.8 which is not representative for UVC-III campaign?**

**Reply**

Data from AERONET indicate that very low SSA values are possible during the campaign. Nevertheless, it is clear in our discussion that this is only a hypothesis since there are no SSA measurements in the UV available.

**327 which denotes that the SSA – which means that the SSA**

**Reply**

Done

**Figure 4. – Suggest moving this figure to supplement. You can use AERONET SSA retrievals on days 197-199.**

**Reply**

We do not agree that this figure should be moved to the supplement since it is useful for the discussion. In the revised version of the manuscript, we also used AERONET SSA in the discussion. However, we cannot draw conclusions that are solely based on the analysis of SSA values from AERONET because 1) SSA at 440 nm is not necessarily fully representative for the SSA in the region 300 – 310 nm (that mostly contributes to the UVI), and 2) because in most cases only the level 1.5 SSA product is available, that is uncertain for very low AOD values. Nevertheless, we analyzed the SSA from AEONET to strengthen our conclusions.

**354-355: Although we have not corrected the modeled UVI for the effect of limited horizon – This horizon correction should be important for Davos site. Quantify this effect using horizon elevation angle as a function of the azimuthal angle.**

**Reply**

We analyze the UVI for SZA greater than  $75^\circ$ , and thus the limited horizon does not affect the direct solar beam. Assuming isotropic diffuse radiation, it has been calculated that the obstacles block about 5% of the diffuse radiation. As discussed in lines 435 – 440, this loss results in an error of less than 2% for the studied cases.

**Figure 8: analysis of the outliers will be useful.**

**Reply**

The following lines have been added (lines 457 – 460):  
“The differences between the UVI from QASUME and the model (with both setups) are in some cases very large, reaching even values of  $\pm 8$ . These large differences are mainly due to the model inability to predict accurately if the fraction of the solar disc that is occluded by clouds, especially under broken cloud conditions.”

**Figure 9. The campaign average difference is close to zero, but there are certain periods (i.e., 200-210) with larger differences. Again, analysis of the largest outliers would increase the value of the comparisons.**

**Reply**

Relevant discussion has been added in the previous sections (3.1 and 3.2) which explains the larger differences. We believe that repeating the same discussion here is not necessary.

**390-400: Section 3.3 is too short. The results in Figure 10 are not discussed. Expand or remove this section.**

## Reply

The discussion in Section 3.3 has been expanded.

**394: when the PMOD/WRC calibration – explain the difference between USER and POD/WRC calibration. Explain if radiometers were calibrated for the non-lambertian angular response (cosine correction)?**

## Reply

Analytical discussion about these issues has been performed in Hülsen and Gröbner, 2023 and Hülsen et al., 2016.

**405 Figure 10: Text in the figure is difficult to read. Try to increase the size of the text or move the text to the caption.**

## Reply

We increased the size of the Figure. Since Figure 10 (now Figure 11) has been provided in high resolution we believe that the text will be readable in the final version.

**426-427: when solar disc is occluded, we do not know the exact COT. – Clarify this sentence.**

## Reply

Done

**436. shows the significance of systematic and accurate calibration of such instruments. – This is true regardless of the model performance ...**

## Reply

The sentence has been deleted

**437 discussed in previous studies – add reference to Fioletov, et al., (2004) “UV index climatology over North America from ground-based and satellite estimates”, J. Geophys. Res., 109, D22308, <http://doi.wiley.com/10.1029/2004JD004820>**

## Reply

Done

**440 associated to the assumptions – with the assumptions**

## Reply

Done

**451 not available (e.g., Bais et al., 2019). – add these references:**

**Krotkov, et al., “Aerosol UV absorption experiment (2002- 04): 2. Absorption optical thickness, refractive index, and single scattering albedo”, Opt. Eng., 44(4), 041005, <http://doi.org/10.1117/1.1886819> , 2005,**

**Corr, Chelsia, et al., “Retrieval of aerosol single scattering albedo at ultraviolet wavelengths at the T1 site during MILAGRO (2009)”, Atmos. Chem. Phys., 9, 5813–5827, <http://doi.org/10.5194/acp-9-5813-2009>**

**Mok, J., et al., “Impacts of atmospheric brown carbon on surface UV and ozone in the Amazon Basin”, Sci. Rep. (2016); <https://doi.org/10.1038/srep36940>**

**Mok, J., et al., “Comparisons of spectral aerosol absorption in Seoul, South Korea”, Atmos. Meas. Tech., 11, 2295-2311, <https://doi.org/10.5194/amt-11-2295-2018>**

**Go, et al., “Ground-based retrievals of aerosol column absorption in the UV spectral region and their implications for GEMS measurements”. Remote Sensing of Environment, 245, 2020, 111759, <https://doi.org/10.1016/j.rse.2020.111759>**

### **Reply**

The recommended references have been added.

# Assessment of the accuracy in UV index modelling using the UVIOS2 system during the UVC-III campaign

Ilias Fountoulakis<sup>1</sup>, Kyriaki Papachristopoulou<sup>2</sup>, Stelios Kazadzis<sup>2</sup>, Gregor Hülsen<sup>2</sup>, Julian Gröbner<sup>2</sup>,  
Ioannis-Panagiotis Raptis<sup>3</sup>, Dimitra Kouklaki<sup>4,5</sup>, Akriti Masoom<sup>2</sup>, Natalia Kouremeti<sup>2</sup>, Charalampos  
5 Kontoes<sup>4</sup>, Christos S. Zerefos<sup>1,6,7,8</sup>

<sup>1</sup>Research Centre of Atmospheric Physics and Climatology, Academy of Athens, 10680 Athens, Greece

<sup>2</sup>Physikalisch-Meteorologisches Observatorium Davos, World Radiation Center (PMOD/WRC), Davos Dorf, Switzerland

<sup>3</sup>Institute for Astronomy, Astrophysics, Space Applications and Remote Sensing, National Observatory of Athens, Greece

<sup>4</sup>Institute for Environmental Research and Sustainable Development, National Observatory of Athens, GR15236 Athens,  
10 Greece

<sup>5</sup>Laboratory of Climatology and Atmospheric Environment, Department of Geology and Geoenvironment, National and  
Kapodistrian University of Athens, 15784 Athens Greece

<sup>6</sup>Biomedical Research Foundation of the Academy of Athens, 11527 Athens, Greece

<sup>7</sup>Navarino Environmental Observatory (N.E.O.), 24001 Messenia, Greece

<sup>15</sup><sup>8</sup>Mariopoulos-Kanaginis Foundation, 10675 Athens, Greece

*Correspondence to:* Ilias Fountoulakis (i.fountoulakis@academyofathens.gr)

**Abstract.** The third campaign for the calibration and intercomparison of solar UV radiometers (UVC III) took place at Davos, Switzerland in June - August 2022. More than 70 radiometers participated in the campaign and measured side-by-side with the portable reference spectroradiometer QASUME. ~~By using inputs from various sources, the UVIOS2 system was used to estimate the UV index (UVI) for the site of the campaign.~~

20 The UVIOS2 system is a flexible UVI modelling tool that can be exploited for different applications depending on the inputs. Thus, different combinations of satellite, reanalysis, and/or

ground-based inputs were used to test the UVIOS2 performance when it is used as a tool for UVI nowcasting or for climatological studies. While UVIOS2 provided quite accurate estimates of the average (for the period of the campaign) UVI levels, larger deviations were found for individual estimates. The average agreement between the UVI from the UVIOS2 and

25 QASUME was better than 1% for all the different sets of inputs that were used for the study. The range of the variability was of the order of 40% for instantaneous measurements (15 min), mainly due to the model's inability to capture the instantaneous

effects of cloudiness, especially under broken cloud conditions. Under clear-sky conditions the model was found to perform much better, with the differences between the model estimates and the QASUME measurements being smaller than 12% for 95% of the studied cases. Even at the pristine environment of Davos, single scattering albedo (SSA) was found to contribute

30 significantly to the modelling uncertainties under cloudless conditions. For relatively small Aerosol Optical Depth (AOD), of the order of 0.2 – 0.4 at 550 nm, the role of the SSA was found to be comparable to the role of AOD in the modelling of the

UVI. ~~Radiometers that were not properly maintained and/or calibrated were found to provide UVI measurements with uncertainty that was comparable to the uncertainty of the UVIOS2 estimates, which highlights the significance of systematic maintenance and calibration of the UV radiometers.~~

35 **1 Introduction**

Exposure to solar ultraviolet (UV) radiation is vital for many living organisms including humans (e.g., Caldwell et al., 1998; Erickson III et al., 2015; Häder, 1991; Häder et al., 1998; Juzeniene et al., 2011; Lucas et al., 2019) but can be harmful when it exceeds certain limits (Diffey, 1991). Exposure of the human skin to UV radiation is the main mechanism that drives the formation of vitamin D, which, in turn, contributes to the strengthening of the immune system (e.g., Lucas et al., 2019; Webb 40 et al., 2022). Moderate exposure to UV radiation has many more benefits for human health that are not related to the formation of vitamin D, such as the contribution to the maintenance of a good mental health and the curation of various skin diseases (Juzeniene and Moan, 2012). Nevertheless, overexposure to UV radiation is the main environmental risk factor for non-melanoma skin cancer, and among the main environmental risk factors for melanoma skin cancer and cataract (WHO, 1994). Determination of optimal sun exposure behaviors is not a simple task and, additionally to the surface solar UV radiation 45 availability, it also depends on the physiology of each individual person (e.g., Armstrong and Cust, 2017; Hoffmann and Meffert, 2005; Lucas et al., 2019; McKenzie and Lucas, 2018; Webb et al., 2018; Webb and Engelsen, 2006).

A commonly used quantity for human health purposes is the UV index (UVI) (Schmalwieser et al., 2017a; Vanicek et al., 2000), which is a metric of the efficiency of UV radiation to cause erythema to the human skin. Generally, smaller exposure times and more precaution measures are recommended with increasing UVI. UVIs smaller than 2 are considered low, UVIs of 50 8 – 10 are considered very high, and UVIs exceeding 10 are considered extreme. In the 1980s and the 1990s, public awareness was caused due to the severe ozone depletion over high and mid latitudes which, if continued, would result in extreme UVI levels over densely populated regions of our planet (van Dijk et al., 2013; Newman and McKenzie, 2011). Although the adoption and the successful implementation of the Montreal Protocol prevented further depletion of stratospheric ozone and the consequent dangerous UV levels (McKenzie et al., 2019; Morgenstern et al., 2008), the future evolution of the levels of 55 surface solar UV radiation is still uncertain, mainly due to the uncertainties in the impact of future climatic~~climate~~ changes on surface solar UV radiation (Bernhard et al., 2023; Zerefos et al., 2023).

Since the 1980s, national and international networks for the monitoring of the UVI have been established to ensure accurate and timely information of the public (Blumthaler, 2018; Schmalwieser et al., 2017). Maintenance of a station that provides reliable UV measurements demands properly trained personnel to run the station and application of strict calibration and 60 maintenance protocols. Furthermore, there are prerequisites for the installation of such stations (e.g., power supply, safety). Thus, it is impossible to achieve UVI monitoring with global coverage from the ground. Progress in satellite monitoring during the last decades allowed the retrieval of the UVI on a global scale. Currently, the UVI has been estimated with high spatial and temporal coverage using various techniques and various satellite products (e.g., see Table 1 in Zerefos et al., 2023). One of the most widely used climatological UVI datasets is provided by the Tropospheric Emission Monitoring Internet Service 65 (TEMIS). TEMIS provides clear-sky UV doses since 1960 and all-sky UV doses since 2004, that have been calculated using measurements from various satellite sensors (<https://www.temis.nl/uvradiation/UVArchive.php>; Zempila et al., 2017). Widely used climatological datasets of the UVI with global coverage have been also retrieved using measurements from the Total

Ozone Mapping Spectrometer (TOMS) (Herman et al., 1999), the Ozone Monitoring Instrument (OMI) (Tanskanen et al., 2006), and the TROPOspheric Monitoring Instrument (TROPOMI) (Lindfors et al., 2018). As a result of the rapid progress in  
70 Earth observation monitoring, the aforementioned climatological satellite-based UV products have been proven to be reliable over wide regions of the planet (e.g., Lakkala et al., 2020; Zempila et al., 2016, 2017), although biases of the order of 10 – 20% have been reported over complex and polluted environments, while uncertainties can be even larger over highly reflective terrains at high latitudes (e.g., Lakkala et al., 2020). The accuracy of satellite-based estimates is ~~mainly limited by due to the~~ the  
75 ~~(Bais et al., 2019b)~~ finite width of the satellite pixel (Kazadzis et al., 2009) and the weakness of satellite sensors to accurately probe the lower troposphere (Bais et al., 2019). In particular, assumptions are made in the satellite algorithms to describe the complex interactions between radiation, aerosols and clouds, which increase the uncertainty in the retrievals. Uncertainties in the assumed aerosol properties (Arola et al., 2021; Parisi et al., 2021), inaccurate distinction of the effect of highly reflecting terrains and cloudiness (Bernhard et al., 2015; Lakkala et al., 2020b), and uncertainties in the description of cloud cover, especially over high-altitude sites (Brogniez et al., 2016; Schenzinger et al., 2023a) are among the main uncertainty sources. ~~bed~~ (Bais et al., 2019b)

Meteorological services provide UVI ~~nowcasting and~~ forecasting that is usually based on meteorological forecasting in conjunction with radiative transfer models (e.g., Feister et al., 2011; Long et al., 1996; Roshan et al., 2020). The Copernicus Atmospheric Monitoring Service (CAMS) ~~- Atmosphere~~ for example, provides five days clear-sky and all-sky UVI forecasts on a global scale based on the synergistic analyses of Earth-observation data, weather prediction and chemistry model forecasts, 85 and radiative transfer modelling (Peuch et al., 2022; Schulz et al., 2022). UVI forecasts are commonly governed by the uncertainties in the forecasted meteorological parameters, mainly cloudiness (e.g., Schenzinger et al., 2023). Geostationary satellites provide continuous, nearly instant information for cloudiness over wide regions of the planet (Derrien and Le Gléau, 2005), which can be used to provide more accurate UVI estimates in nearly real time (Kosmopoulos et al., 2020) or UVI climatological products (e.g., Arola et al., 2002; Fragkos et al., 2024; Verdebout, 2000; Zempila et al., 2017).

90 Monitoring and/or forecasting of the UVI at mountainous sites is exceptionally challenging. Complex atmospheric conditions and complex terrains increase the uncertainties in the modelling of the UVI, while calibration and maintenance of sensors is not easy due to difficulties in access, power supply, and harsh weather conditions. Nevertheless, UVI increases with altitude and can reach extreme levels, which makes this information valuable for the inhabitants and the visitors of such locations. For example, extreme UVI of ~20 has been recorded in the Bolivian Andes (Pfeifer et al., 2006; Zaratti et al., 2003). Elevated UVI 95 levels have been also recorded at high-altitude deserts in Argentina (Piacentini et al., 2003), while UVI frequently exceeding 15 has been measured at Tibet (Dahlback et al., 2007). UVIs frequently exceeding 11 have been also measured at European alpine stations (Casale et al., 2015) as well as at high altitude locations in Northwestern Argentina (Utrillas et al., 2016). Depending on atmospheric and terrain conditions, increases of the surface solar UV radiation levels with altitude can range 100 from a few percent per km (Chubarova and Zhdanova, 2013; Pfeifer et al., 2006; Rieder et al., 2010; Schmucki and Philipona, 2002; Zaratti et al., 2003) to 10-20% (e.g., Chubarova et al., 2016; Sola et al., 2008), or even to more than 30%/km when surface albedo also increases with altitude (Bernhard et al., 2008; Pfeifer et al., 2006). During summer (~~if absence of~~ snow is

absent), UVI increases with altitude mainly due to decreased Rayleigh scattering (Allaart et al., 2004; Blumthaler et al., 1994; Sola et al., 2008). In general, the change in the levels of the solar UV irradiance with altitude depends on atmospheric composition and has a strong wavelength dependence which is introducing difficulties in the modelling of the UVI at mountainous sites (e.g., (Dvorkin and Steinberger, 1999; Krotkov et al., 1998)). At very high-altitude (or/and latitude) sites, ice and/or snow may persist even in late spring and summer resulting in extremely high UV exposure (e.g., (Schmalwieser et al., 2017b; Siani et al., 2008; Utrillas et al., 2016).

The continuous operation of ground-based networks that provide highly accurate information is necessary, not only for the information ~~of to~~ the public, but also for the validation and the improvement of satellite based UVI climatological and forecast/nowcast products (e.g., Fountoulakis et al., 2020b). In addition to the strict maintenance, operation, and calibration protocols that must be applied by the monitoring stations operators (e.g., Fountoulakis et al., 2020a; Garane et al., 2006; Gröbner et al., 2006; Lakkala et al., 2008), participation of the instruments to field campaigns further ensures the high quality and the homogeneity of the measured UVIs at different stations (Bais et al., 2001; Hülsen et al., 2020). The uncertainty in the UVI measured by the most accurate spectroradiometers that serve as world references can reach 2% (Gröbner and Sperfeld, 2005; Hülsen et al., 2016). Broadband filter radiometers that are commonly used in regional, national, or international networks for UVI monitoring are affected by larger uncertainties. In the context of the solar ultraviolet filter radiometer comparison campaigns (UVC, UVC-II, and most recently UVC-III) that were organized by the Physikalisch-Meteorologisches Observatorium Davos, World Radiation Center (PMOD/WRC) in 2006, 2017, and 2022 many broadband radiometers measured side-by-side with the world reference QASUME (e.g., Hülsen et al., 2020; Hülsen and Gröbner, 2007). Analyses of the measurements by the 75 instruments that participated in UVC-II resulted in the estimation of a calibration uncertainty of 6%. The overall uncertainty in the measurements was larger, due to other factors, mainly the imperfect angular response of the radiometers (Hülsen et al., 2020).

Furthermore, Davos is one of the few mountainous sites in the world where both, highly accurate UVI measurements, and measurements of the main factors that determine the levels of the UVI at the surface (and can be used as inputs for its modelling) are available, which allows us to assess the efficacy of a state-of-the-art UVI model to produce estimates and reconstructed UVI series under such conditions.

The first version of the UVIOS (UV-Index Operating System) nowcasting system ~~that its basic features have has~~ been already described in Kosmopoulos et al., (2021). The system has been upgraded recently in order to achieve faster and more accurate simulations. The new, improved UVIOS2 radiative transfer scheme can be used either as a tool for UVI ~~nowcasting and~~ forecasting or for climatological studies, depending on the inputs. In this paper, the UVI that has been simulated using the new UVIOS2 system with different inputs is described and validated against very accurate ground-based UVI measurements that were performed during the UVCIII campaign. The world reference QASUME that operated during the campaign provides measurements that are ideal for the validation of UVIOS2 due to their high accuracy, which allows the identification of the uncertainties in the modelling of UVI by UVIOS2. Highly accurate ancillary measurements that were available at the same

135 period also allow the identification of the uncertainty sources in the UVI modelling. The main targets of the study can be summarized as follows:-

- Describe the upgrades in UVIOS2 relative to the previous (UVIOS) system.
- Quantify the uncertainties, and the main uncertainty factors, in UVIOS2 simulations during the UVCIII campaign, when it is used as a tool for UVI nowcasting and climatological analysis.
- 140 - Evaluate and discuss in depth the uncertainty factors in the modelling of UVI at complex topography sites such as Davos.
- Discuss the uncertainty in forecasted UVI with respect to the uncertainty in the measurements of filter radiometers and discuss what are the prerequisites for improved UVI modelling.

145 It must be clarified that the study refers to a snow-free period at Davos, and thus the uncertainties related to the parameterization of surface albedo, which may be significant for higher altitude sites even in the summer, are not quantified or discussed here.

The paper is organized as follows. A description of the used data and methods is provided in Section 2. The results of the analysis are discussed in Section 3, and the main conclusions are summarized in Section 4.1.1 Subsection (as Heading 2).

## 2 Methodology

The UVIOS2 system is a flexible tool that can be exploited for different applications depending on the inputs. It can be used either as a nowcasting/forecasting tool, or to perform climatological studies. The accuracy of the simulated UVI depends on 150 the compromise between the achievement of realistic computational times (i.e., the spatial and temporal extent of the simulations) and the use of the most accurate model inputs. In the context of this work, we assessed the accuracy of UVIOS2 when it operates for real time applications (i.e., default setup that is used to simulate the real-time UVI over Europe) and when it is used for climatological studies (i.e., using ground-based measurements or reanalysis data as inputs) at the mountainous environment of Davos, Switzerland during the UVC III campaign (Hülsen and Gröbner, 2023). Assessment of the accuracy in 155 UVIOS2 forecasts is out of the scope of the present study.

### 2.1 The UVC-III campaign

The third International Solar UV Radiometer Calibration Campaign (UVC-III) took place at Davos, Switzerland (Figure 1; 46.8°N, 9.83°E, 1610 m a.s.l.) from 13 June to 26 August 2022, and was organized by the PMOD/WRC as part of the 160 WMO/GAW program (Hülsen and Gröbner, 2023). The QASUMEII data (see Sect. 2.2) ~~was~~were used as reference for the calibration of the broadband radiometers during the campaign. QASUME and QASUMEII were frequently calibrated during the campaign using a portable calibration system with 250 W lamps. The two spectroradiometers remained stable within ±1% for the campaign period and their measurements differed by less than 3%. Seventy-five solar UV broadband filter radiometers were shipped to Davos and participated in the campaign. The UVI ~~measured by the participating instruments~~ was derived from the measurements of the participating instruments using the calibration factors provided by the operators and the calibration 165 factors that were calculated at Davos, and then the ~~measurements~~UVI from the radiometers ~~were~~was compared to the UVI measured by QASUMEII. All participating instruments were also characterized for their angular and spectral response.

Ancillary measurements of many parameters that are valuable for the determination of the factors that result in discrepancies between the simulations of UVIOS2 and the measurements were performed during the whole period of the campaign. In particular:

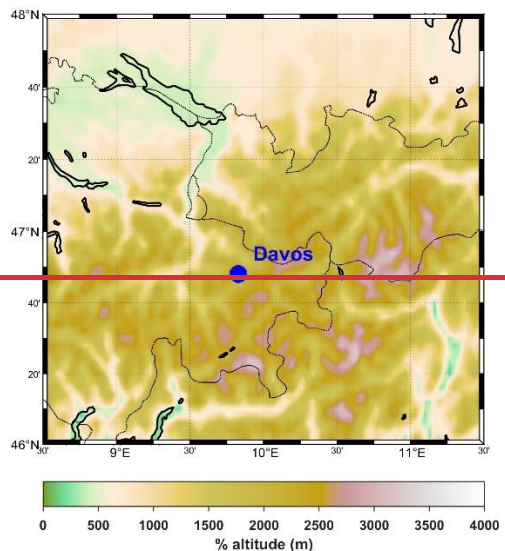
170 - Aerosol optical properties were measured by a CIMEL radiometer (and many other radiometers that operate at the site) that is part of the AERONET network (Holben et al., 1998).

- Total Ozone Column (TOC) was measured by a Brewer spectroradiometer (Kerr, 2010; Kerr et al., 1985).

- Global and direct total solar irradiance by pyranometers and a pyrheliometer.

175 - Hemispherical sky images from sky cameras.

- Cloud cover in octas by a pyrgeometer (Dürr and Philopona, 2004)



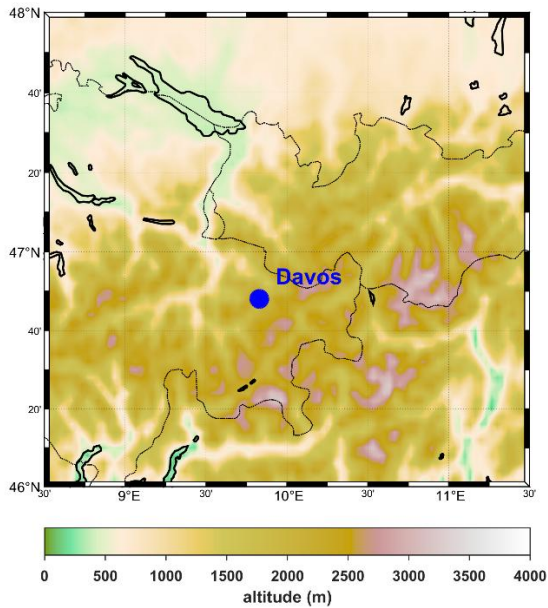


**Figure 1. Topographical map of Davos, Switzerland.**

180 **2.2 QASUME**

QASUME is a transportable spectroradiometer that is traceable to the scale of spectral irradiance established by the Physikalisch-Technische Bundesanstalt (PTB) and serves as [a reference](#) for spectral solar UV irradiance. The system is maintained by the PMOD/WRC and its measurement accuracy has been improved significantly in the last two decades. [Since 2014, a second reference spectroradiometer \(QASUMEII\) is also operating and is used as an additional reference standard](#)

185 (Hülsen et al., 2016). Upgrades of technical characteristics and improved characterization methodologies have reduced the expanded uncertainties in QASUMEII measurements at wavelengths above 310 nm from 4.8 % in 2005 [\(for QASUME\)](#) to 2.0 % in 2016 (Hülsen et al., 2016). More information about QASUME [and QASUME II](#) can be found in several relevant studies (Gröbner et al., 2005, 2006; Gröbner and Sperfeld, 2005; Hülsen et al., 2016). [Since 2014, a second reference spectroradiometer \(QASUMEII\) is also operating and is used as an additional reference standard \(Hülsen et al., 2016\)](#). Both, 190 QASUME and QASUMEII were measuring in the range 290 – 420 nm with a 15 min temporal resolution during the UVC-III campaign. These spectra were weighted with the erythema action spectrum (Webb et al., 2011) and were then integrated to calculate the erythema doses, and subsequently the UVI (by dividing the [doses](#) in  $\text{mW/m}^2$  with 25). For this work we have

used only the UVI measured by QASUMEII, since the agreement between QASUMEII and QASUME is better than 3%. QASUMEII is ~~referred~~<sup>referred to</sup> as QASUME throughout the manuscript

195 **2.3 The UVIOS2 system**

UVIOS2 is built upon the UVIOS system (Kosmopoulos et al., 2021). The main change in the system configuration relative to the previous version is that the UVI is calculated in two steps:

- (i) the UVI is calculated under cloudless ~~clear~~ skies and
- (ii) the effect of clouds is quantified as a second step for the calculation of the all-skies UVI.

200 This change in the system's configuration was accompanied by two major modifications/upgrades: (1) the use of a more detailed UV look up table (LUT) for ~~clear~~<sup>cloudless</sup>-sky calculations that increases the accuracy relative to the original version, and (2) the use of the UV cloud modification factor (CMFUV) concept used for the all skies UVI estimates. The variables that correspond to each of the five different dimensions of the LUT are listed in Table 1, along with their range and resolution. When SZA exceeds 89°, then UVI is considered equal to 0. When values of the other input parameters are above/below the 205 limits shown in Table 1, then inputs are set to the upper/lower values of the used range. Such occasions are, however, very rare for mid-latitude sites.

**Table 1. Inputs of the LUT**

Parameter	Range	Resolution
SZA (°)	1 - 89	2
TOC (DU)	200 – 600	10
AOD at 550 nm	0 - 2	0.1
SSA	0.6 - 1	0.1
AE	0 – 2	0.4

210 The radiative transfer simulations for the creation of the LUT were performed using the UVSPEC model of the libRadtran package (Emde et al., 2016; Mayer and Kylling, 2005). Simulations were performed using the National Infrastructures for Research and Technology (GRNET) High Performance Computing Services and the computational resources of the ARIS GRNET infrastructure. Spectral simulations per 0.5 nm were performed for the spectral region 290 nm – 400 nm, using the atlas plus modtan extraterrestrial spectrum ([ETS](#)) and the sdisort solver (Dahlback and Stamnes, 1991) which assumes pseudospherical atmosphere. [Using a different ETS might result to differences in the simulated erythema irradiances, as for example was shown in the study of](#) [Gröbner et al., \(2017\)](#). [Based on the results of the latter study we estimate that the simulated irradiances might differ by up to 5% if a different ETS was used, making the used ETS spectrum a major uncertainty factor in UVIOS2 simulations.](#) The default libRadtran absorption cross-sections of species that absorb radiation in this spectral region (mainly O3, SO2, and NO2) were also included. [TOC is among the main regulators for the UVI levels at the surface and thus](#)

220 using TOC values that have been retrieved using different ozone absorption cross sections relative to those that have been used to create the LUT (Molina and Molina, 1986) would result in differences between the measured and the simulated UVI. Differences of 1 - 3% have been reported in the retrieved TOC depending on the used absorption cross sections (Fragkos et al., 2015; Redondas et al., 2014), which may result in differences of up to ~5% in the calculated UVI, depending mainly on the used cross sections, the SZA, aerosols load, and cloudiness (Blumthaler et al., 1995; Kim et al., 2013). In the domain for which the system is commonly used (i.e., Europe, North Africa, Middle East), variability in SO<sub>2</sub> and NO<sub>2</sub> has a minor impact 225 on the UVI, and thus default values of their total concentration have been used. The US standard atmosphere (Anderson et al., 1986) was used to describe the profiles of atmospheric state and composition, and the surface albedo was set to 0.05. Adjustment of the surface albedo to the local conditions when UVIOS is used over more reflective terrains (e.g., deserts, snow-covered surfaces) is within the model improvements that are planned for the future since under such conditions assuming a standard value of 0.05 could result in large uncertainties (e.g., Weihs et al., (2001)).

230 The profiles of libRadtran default aerosol model (Shettle, 1990) were scaled to the values of AOD (spectrally using the corresponding Ångström Exponent, AE) and SSA provided in Table 1. We did not consider the spectral dependence of the absorbing aerosol optical depth (as e.g., in the OMI and TROPOMI algorithms (Arola et al., 2021)), which may induce increased uncertainties over polluted regions (e.g., Roshan et al., (2020)). However, considering such information would increase significantly the size of the LUT and thus the computational time needed for the simulations, making the provision of 235 the UVI in near-real time for wide areas impossible.

The UV spectra were weighted with the action spectrum for the induction of erythema in the human skin (Webb et al., 2011) to calculate the UVI. A correction for the effect of altitude, assuming an increase of 5% per km (e.g., Zempila et al., 2017) has been applied on the calculated UVI.

240 The cloud optical thickness (COT) from the Spinning Enhanced Visible and Infrared Imager (SEVIRI) instrument aboard the Meteosat Second Generation (MSG) satellites has been used to calculate the CMF. The COT product is extracted operationally using the EUMETSAT Satellite Application Facilities of Nowcasting and Very Short-Range Forecasting, NWC SAF software package (Derrien and Le Gléau, 2005; Météo-France, 2016) and the broadcasted MSG data. A detailed description of the cloud products by MSG can be found in the relevant bibliography (Deneke et al., 2021; Météo-France, 2016). Using the MSG COT values and the SZA as inputs to the multiparametric equations described in Papachristopoulou et al. (2024) the shortwave CMF 245 is calculated. Then, it is converted to CMFUV as described in Staiger et al. (2008). Finally, the UVI is calculated by multiplying the clearcloudless-sky values with the CMFUV. Using cloud optical thickness to simulate UV instead of using the CMFUV might be more accurate (Krotkov et al., 2001), but would increase computational time, and still the dominant uncertainty factor related with cloudiness would be the visibility of the solar disc.

250 To evaluate the methodology used for the quantification of the attenuation of the UVI by clouds the all-sky UVI was compared to QASUME measurements. Furthermore, the all-sky UVIs were compared to the corresponding values that were directly simulated by using cloud optical properties as inputs in the UVSPEC model of libRadtran. It was assumed that all low-altitude clouds over Davos extend from 4 km to 5 km (with reference to the a.s.l.), and all high-altitude clouds extend from 7 km to 8

km. High-altitude clouds were in all cases assumed to consist of ice crystals with effective radius equal to 20  $\mu\text{m}$  and ice water content (IWC) of 0.005 g  $\text{cm}^{-3}$ , while low-altitude clouds were assumed to consist of water droplets with effective radius equal to 10  $\mu\text{m}$  and liquid water content (LWC) value of 1 g  $\text{cm}^{-3}$ . The COT at 550 nm product from MSG was used as an additional input, which leads to an adjustment of the default LWC and IWC values, using the parameterizations by Hu and Stamnes (1993) for water and by Fu (Fu, 1996; Fu et al., 1998) for ice clouds. The latter simulations were performed for the altitude of the site, while all other model settings were the same as those used to produce [the LUT](#). The simulations that were performed for the altitude of the site were also used to evaluate the assumption that the UVI increases by 5% per km.

Practically there are two ways of using UVIOS2. For past data using the best available information giving priority to ground based/satellite based/modelling based data in this order of preference. For nowcasting or short term forecasting using any existing real time available data.

**Table 2. Inputs of the UVIOS2, TEMIS, and CAMS services that provide the UVI.**

Parameter	UVIOS2	TEMIS	CAMS
<u>Past/reanalysis data</u>			
<u>Cloud inputs</u>	Based on MSG Cloud Optical thickness	Cloud correction based on satellite data (reflectivity, cloud cover).	Dynamic cloud modeling with real-time weather forecasts.
<u>Spatial</u>	5km x 5km for clouds 13 km x 24 km for Ozone	~80 km x 40 km (GOME-2) to 13 km x 24 km (OMI).	0.4° x 0.4° (~44 km x 44 km).
<u>Temporal</u>	Every 15 minutes	Daily updates (based on satellite overpasses).	Every 1 hour
<u>Aerosol</u>	Ground based measurements or CAMS AOD, based on availability at the location under study	Through cloud reflectivity or historical AOD	advanced atmospheric models and data assimilation from satellite and ground-based observations.
<u>Total ozone</u>	Brewer if available, mainly based on OMI	Based on OMI	Full atmospheric modeling (transport + chemistry).
<u>Nowcast/forecast data</u>			

<u>Cloud inputs</u>	<u>Based on MSG Cloud Optical Thickness and cloud motion vectors (for forecast)</u>	<u>Not available forecasts.</u> <u>Only Cloudless sky UV</u>	<u>Dynamic cloud modeling with real-time weather forecasts.</u>
<u>Spatial</u>	<u>5 km x 5 km for clouds</u> <u>13 km x 24 km for Ozone</u>	<u>~80 km x 40 km (GOME-2) to 13 km x 24 km (OMI).</u>	<u>0.4° x 0.4° (~44 km x 44 km).</u>
<u>Temporal</u>	<u>Every 15 minutes up to 3 hours</u>	<u>Daily up to 7 days</u>	<u>Every 3 hours up to 5 days</u>
<u>Aerosol</u>	<u>Based on CAMS AOD forecasts</u>	<u>Historical AOD</u>	<u>CAMS forecasting</u>
<u>Total ozone</u>	<u>TEMIS forecast used (previous day)</u>	<u>TEMIS forecast: Based on satellite observations with some basic extrapolation techniques</u>	<u>Uses multiple satellite sources + numerical models.</u>

265 As shown in Table 2 there are basic differences but also common approaches in the three UVI services. The main advantage of UVIOS2 is that it provides higher spatiotemporal resolution for nowcasted or past data. Nevertheless, it utilizes CAMS and TEMIS forecasts for AOD and ozone nowcasts/forecasts respectively. Overall, all the data used are going through libRadtran towards calculating UVI.

## 2.4 UVIOS2 inputs

270 Different combinations of model inputs have been used to assess the UVIOS2 accuracy when it is used for nowcasting and for climatological analyses. In all cases, the modelled ~~clear~~cloudless-sky UVI values were derived by interpolating linearly the elements of the 5-dimensional LUT. An overview of the data that was used to interpolate the UVI is presented in Table 23.  
 In all cases, default values of the aerosol asymmetry parameter (ASY) and the surface albedo were used for the simulations. Analyses of different AERONET datasets shows that climatological ~~asymmetry parameter~~ASY at 440 nm usually varies by about  $\pm 0.03$  around a typical value that is slightly lower than  $\sim 0.7$  (e.g., Fountoulakis et al., 2019; Kazadzis et al., 2016; Khatri et al., 2016; Raptis et al., 2018). Given that ASY generally ~~de~~increases with wavelength it was assumed to be 0.7 in the UV. The real ASY can however differ occasionally by up to about  $\pm 0.1$  (e.g., Fountoulakis et al., 2019). We estimated that a difference of 0.1 in the asymmetry parameter can result in differences of up to  $\sim 2\%$  in the simulated UVI. Using a default surface albedo (0.05) also introduces uncertainties in the modelling of the UV index. Surface albedo changes spectrally

280 and its impact differs depending on aerosol load and properties (e.g., Corr et al., 2009; Fountoulakis et al., 2019). Nevertheless, during the snow-free period at Davos differences in surface albedo are estimated to be within  $\pm 0.03$  (e.g., Feister and Grewe, 1995) resulting in differences that are of the order of a few percent. ~~-~~ Sensitivity analysis revealed that the uncertainty in the UVI simulations for  $AOD \leq 0.5$  due to the combined effect of using default ASY and surface albedo values (with errors of  $\pm 0.1$  and  $\pm 0.03$  respectively) is less than 3%.

285

Table 23. Combinations of input data for the UVIOS2 system for cloudless sky conditions. The three different combinations used to evaluate the system as a tool for climatological analysis are referred to as CAMS, CAMS+OMI, GB.

Variable	Nowcasting I (SAT)	Climatological I (CAMS)	Climatological II (CAMS+OMI)	Nowcasting II and Climatological III (GB)
<b>AOD</b>	CAMS forecasted AOD at 550 nm	CAMS reanalysis AOD at 550 nm	CAMS reanalysis AOD at 550 nm	Measured AOD at 500 nm from CIMEL
<b>TOC</b>	Forecasted from TEMIS	CAMS reanalysis	OMI measured	Measured from Brewer
<b>AE</b>	Climatological (1.5)	Climatological (1.5)	Climatological (1.5)	Measured by CIMEL (440 – 675 nm)
<b>SSA</b>	<del>Climatological (0.9)</del>	<del>Climatological (0.9)</del>	<del>Climatological (0.9)</del>	<del>Climatological (0.9)</del>
<b>ASY</b>	<del>0.7</del>	<del>0.7</del>	<del>0.7</del>	<del>0.7</del>
<b>Surface albedo</b>	<del>0.05</del>	<del>0.05</del>	<del>0.05</del>	<del>0.05</del>

290 For UVI nowcasting, ~~the aerosol properties and TOC that were used as model inputs were either forecasted forecasts (AOD, TOC) and/or climatological datasets were used as inputs for aerosol parameters values (AE, SSA, ASY) and TOC~~. Specifically, 1-day ahead forecasts of the TOC from TEMIS (<https://www.temis.nl/uvradiation/nrt/uvindex.php>) and of the AOD at 550 nm from CAMS (<https://ads.atmosphere.copernicus.eu/cdsapp#!/dataset/cams-global-atmospheric-composition-forecasts?tab=overview>), as well as monthly climatological values of the SSA and the AE (typical values of 0.9 and 1.5, respectively, have been estimated for Davos) were used to interpolate the elements of the LUT. Total ozone 5-days ~~ahead~~ forecasts are available from TEMIS on a daily temporal resolution. Detailed description of TEMIS and the available products can be found on the service web-page (<https://www.temis.nl/uvradiation/product/index.php>). The CAMS forecasted AOD is available for the following 5 days, on a 1-hour resolution, and the forecasts are updated every 12 hours.

For the calculation of the climatological ~~clear~~~~cloudless~~-sky UVI, the three combinations of inputs presented in Table 2-3 were used:

300 (1) Reanalysis TOC and AOD from CAMS (Inness et al., 2019) instead of the corresponding forecasted products. All other parameters were kept the same as for nowcasting. The CAMS reanalysis, available from 2003 onwards, is the global reanalysis dataset of atmospheric composition of the European Centre for Medium-Range Weather Forecasts (ECMWF), consisting of three-dimensional time-consistent atmospheric composition fields, including aerosols and chemical species. It is based on ECMWF's Integrated Forecast System (IFS), with several updates to the aerosol and chemistry modules described by Inness et al., (2019). CAMS reanalysis products are available from the Copernicus Atmosphere Data Store (ADS, <https://ads.atmosphere.copernicus.eu/#/home> (last access on 8 August 2024)) on a 3-hourly basis on a regular  $0.75^\circ \times 0.75^\circ$  latitude/longitude grid (instead of their native representation).

305 (2) TOC that has been retrieved from the Ozone Monitoring Instrument (OMI) aboard Aura (Levelt et al., 2006), and reanalysis AOD from CAMS (Inness et al., 2019). All other parameters were again kept the same as for nowcasting.

310 (3) TOC measurements from the Brewer spectroradiometer with serial number 163 (Brewer#163) (Gröbner et al., 2021), AOD at 500 nm, and AE (440 – 675 nm) from the CIMEL radiometer (Giles et al., 2019), and all other parameters the same as for the default nowcasting setup. The AOD and AE that were used for the study are level 1.5, version 3 AERONET direct sun products. Level 2 AERONET retrievals were not used because they ~~are~~~~were~~ not available ~~yet~~~~at the time of the analysis~~. Since these inputs are produced in ~~nearly~~ real time, we consider that they could be potentially used for UVI nowcasting in addition 315 to climatological studies. Level 2 AERONET retrievals are available with a longer latency and can be used for reanalysis at a later stage.

The ~~clear~~~~cloudless~~-sky UVI LUT outputs were in all cases post corrected for the effect of the varying Earth-Sun distance and for the surface elevation (1596 m for Davos). The all-sky UVI values were derived in all cases by multiplying the ~~clear~~~~cloudless~~-sky UVI with the Cloud Modification Factor in UV (CMFUV), which was calculated as described in Sect. 2.1 320 from the MSG-SEVIRI COT.

The UVI was simulated for the period 1 July – 20 August 2022 at the time of the QASUME measurements (15 min temporal resolution). The MSG images, and thus the CMFUV, were available at the exact time of the UV scans. All the other parameters (AOD, TOC, etc) were interpolated linearly to the time of the measurements.

For the analysis, measurements were classified as clear-sky (i.e., sun was not fully or partially covered by clouds) and all-sky 325 (i.e., for all cloudiness conditions). In the following, clear-sky conditions refer to unoccluded solar disc according to measurements (although clouds may be present on the sky). Cloudless-sky conditions refer to cloud-free skies. To classify the measurements, the direct component of the total solar irradiance, as it was measured by the pyrheliometer that was operating at Davos during the campaign, was simulated as described in Papachristopoulou et al. (2024), and was then compared to the measured direct irradiance. When differences between the two components exceeded 10%, we considered that the sun was 330 (fully or partially) covered by clouds.

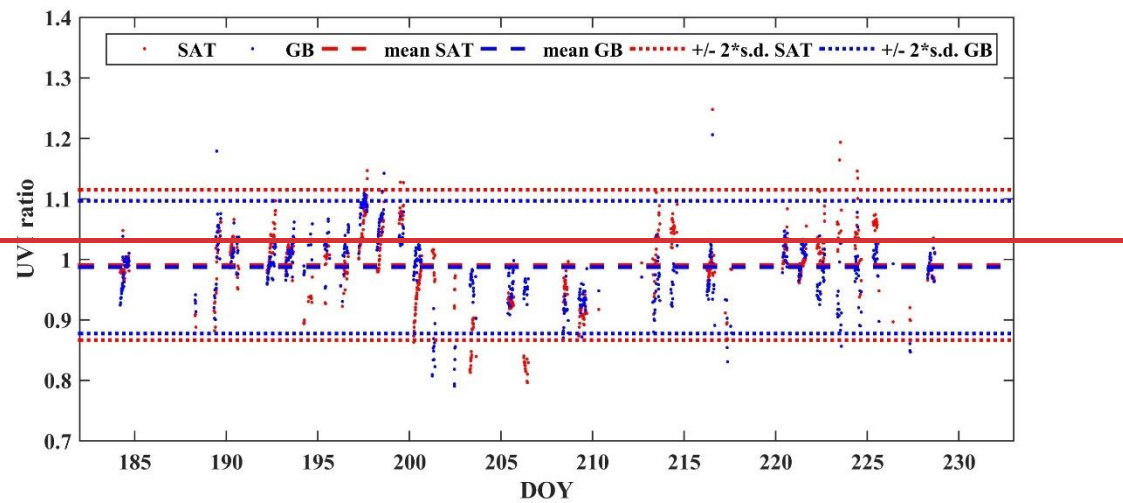
### 3 Results

#### 3.1 Assessment of UVIOS2 for real time applications

In this section we tried to assess the accuracy of the modelled UVI when UVIOS2 is used for real time applications. Initially we compared the modelled and the measured UVI under clear-sky and all-sky conditions. The UVI was modelled using the 335 default inputs and setup of the UVIOS2 (SAT), as well as using high quality ground-based measurements (GB), that theoretically can be available at near real time for the retrieval of a higher accuracy estimate of the UVI.

##### 3.1.1 Clear-sky UVI

Under clear-skies, the ratio between ~~both~~ modelled UVI datasets and the corresponding measured UVI from QASUME~~7~~ was then calculated~~7~~ and the results are shown in Fig. 2.



340

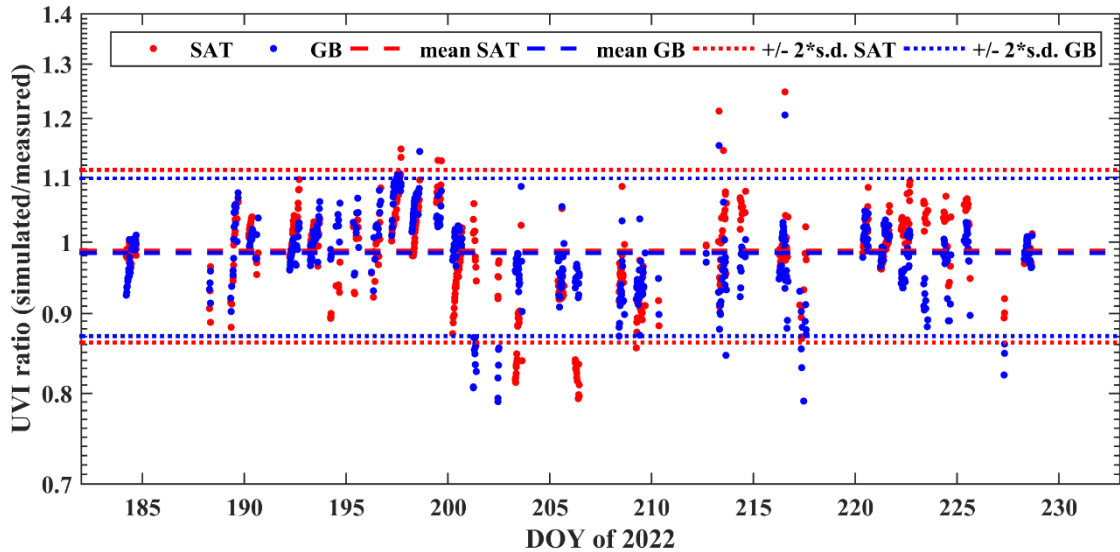


**Figure 2. Ratios between simulated and measured clear-sky UVI.** Red colour: ratios for simulations performed using forecasted CAMS AOD and TEMIS TOC. Blue colour: ratios for simulations performed using measured AOD, AE (by CIMEL), and TOC (by Brewer). Ratios have been calculated for SZA < 75°. Dashed lines represent the mean, while dotted lines represent the range of 2 standard deviation.

While the average ratio is in both cases ~0.99, the standard deviation is high, 0.062 and 0.055 for SAT and GB respectively, i.e., only slightly lower for GB. This result shows that using highly accurate inputs for TOC, AOD at 500 nm, and AE does not result in a noticeable improvement in the accuracy of the average modelled clear-sky UVI (standard deviation decreases by only a few percent), which denotes that other factors are also important for the formulation of the surface UVI levels at Davos. The role of each of the factors that were found to be the most important is discussed in the following.

**AOD and TOC:** The AOD forecasted by CAMS is at a different wavelength (550 nm) relative to the AOD measured by the CIMEL (500 nm). To compare the AOD from the two different sources, the AOD from the CIMEL was extrapolated at 550 nm using the measured AE (440 – 675 nm). The differences between the AOD at 550 nm from the CIMEL and CAMS are shown in the Appendix (Figure A1). Differences in AOD are in all-most cases within  $\pm 0.1$ , with an average of ~0, which explains differences of up to about  $\pm 10\%$  between the UVIs simulated using the two different datasets. When differences in AOD are larger (e.g., in day of the year (DOY) 201 – 202 CAMS has not captured the large AOD levels over the site and the AOD from CAMS is lower by 0.15 – 0.25 relative to the AOD from CIMEL) they result in correspondingly larger differences between the ratios (of 10 – 20%). Differences in TOC (Figure A2 in the Appendix) are generally within  $\pm 25$  DU, with an average of about  $-4$  DU (on average, TEMIS slightly underestimates overestimates TOC for the period of the campaign), but occasionally they can reach  $\pm 40$  DU. Differences of  $\pm 25$  DU in TOC can justify differences of about  $\pm 15\%$  in the UVI modelled using the two different datasets (e.g., Kim et al., 2013). The large differences between the ratios that were calculated for the two different UVI datasets in day of year (DOY) 194 are mostly explained by differences in TOC (~20 DU during most

of the day). Differences in DOYs 200 – 204, 206, and 223 are mostly explained by differences in AOD. The accuracy in the 365 ground-based measurements ( $\sim 0.02$  for the AOD (Giles et al., 2019) and better than 2.5% for TOC (e.g., Carlund et al., 2017; Fountoulakis et al., 2019) cannot justify the standard deviation of 0.055 in the ratio between the modelled UVI when GB measurements are used as inputs and the measured UVI.

**SSA:** While a default SSA value of 0.9 has been used for the simulations, the real SSA at the shorter UV wavelengths, which contribute the most in UVI, can differ significantly, ranging from values smaller than 0.8 (during e.g., events of dust, **polluted** 370 or biomass burning aerosols that have been transferred over the site) to values exceeding 0.98 (e.g., for mixtures that are dominated by sulfuric aerosols). The sensitivity of the ratios **shown in Figure 3** to the **used** SSA increases with increasing AOD as shown in **Figure 3**. For AOD between 0.3 and 0.4 a change of 0.1 (increase or decrease) in SSA results in a change of  $\sim 0.1$  in the ratio (i.e.,  $\sim 10\%$  in the simulated UVI) which is of similar magnitude with the change in UVI due to a change of  $\sim 0.1$  in AOD. The effect of changing SSA becomes less significant as the AOD decreases. Nevertheless, even for AOD of  $\sim 0.1$ , a 375 change of  $\sim 0.1$  in the SSA results in a change of 0.05 in the ratio (i.e., of  $\sim 5\%$  in the modelled UVI). Generally, Figure 3 denotes that aerosol mixtures over Davos in the summer are dominated by aerosols that are weak absorbers of the UV radiation.

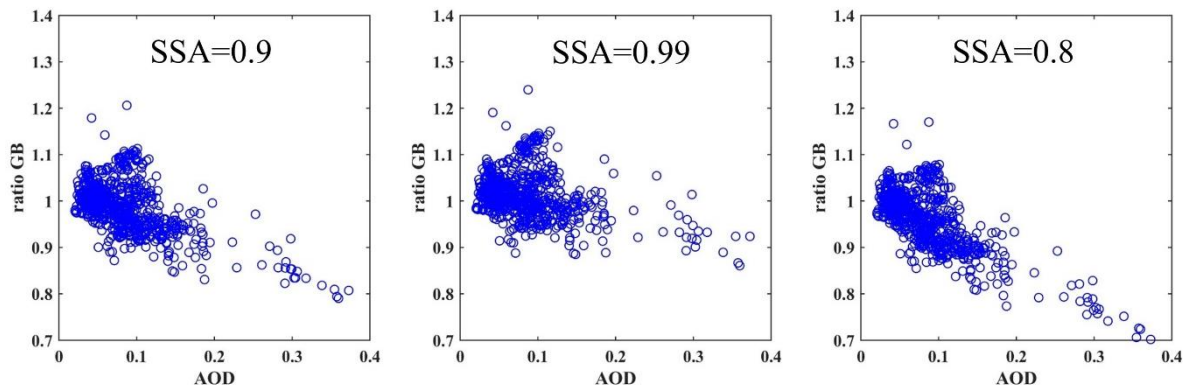


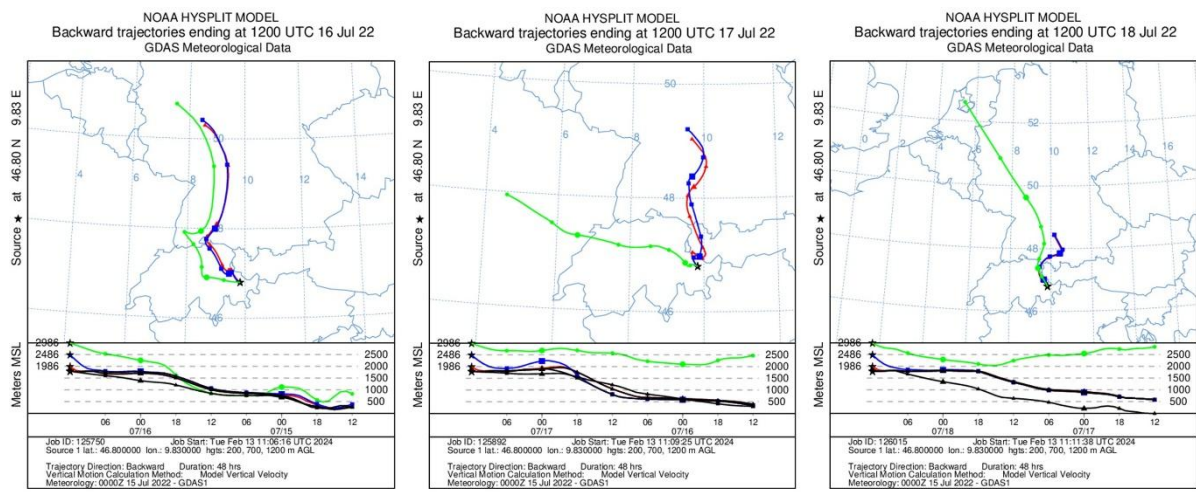
**Figure 3. Ratios between simulated (using GB measurements) and measured clear-sky UVI when different SSA values are used for the simulations.**

380 Changing the SSA from 0.8 to 0.99 results in mean ratio values that are similar to each other and close to unity (see Figure A3 in the appendix) **an SSA of 0.99 results in the median ratio value ( $\sim 1.01$ )**. Nevertheless, using SSA=0.9 results in a distribution of the ratio that is more symmetrically **distributed** around the mean and closer to normal (see Figure A3 in the appendix), which **denotes means** that the SSA of 0.9 is more representative of the average conditions at Davos, at least during the campaign.

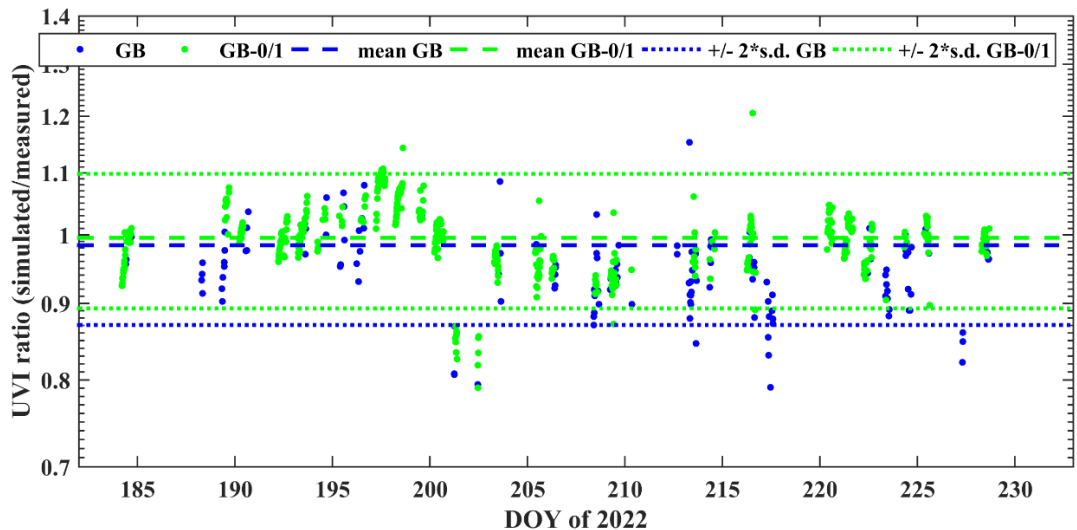
The high values of the ratios between modelled and measured UVIs in DOYs 197 – 199 can be possibly justified by real SSA 385 values that are lower than 0.9, and thus assuming SSA=0.9 for the simulations results in an overestimation of the UVI. **In these days, the SSA at 440 nm from AERONET was generally lower than 0.9 (values between 0.77 and 0.92)**. As shown in Figure 4, **the low SSA values may be due to** air masses that **possibly** transfer polluted aerosols from lower altitudes at Germany **were present over Davos in these days**. **During DOY 200 – 210 when a negative bias is evident in Fig. 2, in addition to the broken cloud conditions that occasionally enhanced significantly the real UVI (see the discussion below), high levels of scattering**

390 aerosols were recorded over Davos (AOD at 340 nm from AERONET was  $\sim 0.6$  in DOY 201-202, and SSA at 440 nm was generally above 0.97). We were not able to identify the conditions that favoured the presence of such high loads of reflective aerosols at the region. In DOY 201 and 202 the AOD is underestimated by CAMS by up to 0.25 (Fig. A1). Nevertheless, in these days the agreement between the measured and modelled UVI is much better for SAT (simulated using CAMS AOD) relative to GB. By comparing CIMEL AOD measurements with measurements from other photometers we confirmed that they are accurate. As shown in Fig. 5, broken cloud conditions during these days cannot explain the UVI enhancement (as e.g., in DOY 217). When the CAMS AOD data were used to simulate the UVI, errors in the AOD and the AE possibly counterbalanced the large errors due to the SSA which possibly resulted in better agreement between the modelled and the measured UVI for the particular dataset (see Fig. 2).

395

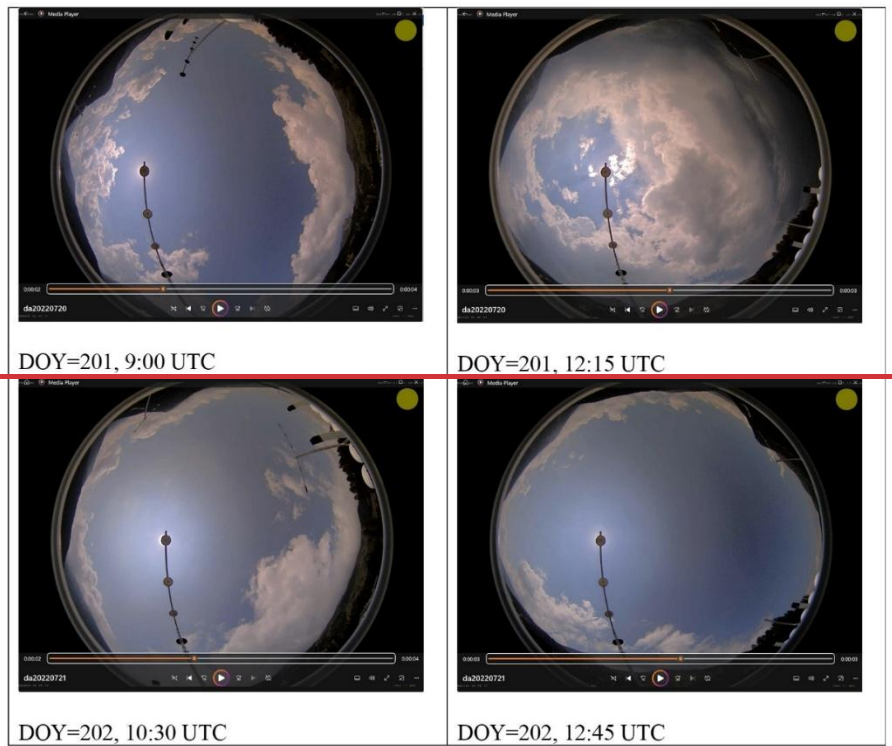


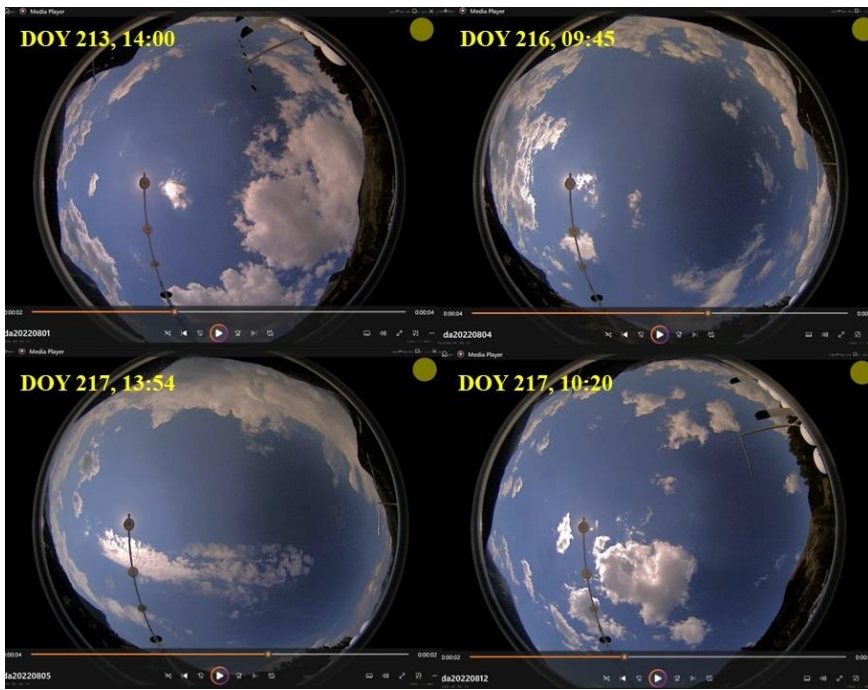
400  
Figure 4. HYSPLIT back-trajectories of the air masses that arrived over Davos (at altitudes 400, 900, and 1400 m over the site).



**Figure 5. Ratios between simulated and measured clear-sky UVI for simulations performed using measured AOD, AE (by CIMEL), and TOC (by Brewer). Blue color: Unoccluded sun with cloudiness in the sky between 0 and 7 octas. Green color: Unoccluded sun with cloudiness in the sky between 0 and 1 octas.**

405





410 **Figure 56.** Sky camera images for [different DOYs 201 and 202 and times](#), which show the clouds near the sun that enhance the UVI at the surface.

Clouds near the sun that do not cover the solar ~~disk~~<sup>disc</sup>: At high altitude stations such as Davos, the presence of orographic clouds is frequent [\(some examples are shown in Fig. 6\)](#). Such clouds can enhance the UVI at the surface if they do not cover 415 the solar disc, by redirecting part of the diffuse irradiance to the surface. [Using the GB UVI dataset we tried to assess the impact of the presence of clouds when the sun is unoccluded. By comparing the ratios when there are very few or no clouds in the sky \(unoccluded sun, 0 or 1 octas, green points in Fig. 5\) with the ratios for all cloudiness conditions \(unoccluded sun, 0 - 7 octas, blue points in Fig. 6\) we confirm that including conditions with 2-7 octas adds a small negative bias in the ratio, possibly due to the enhancement by clouds. Removing these cases slightly improves the ratio and reduces the variability.](#)

420 [In DOYs 201 and 202 the AOD is overestimated by CAMS by up to 0.25. Nevertheless, in these days the agreement between the measured and modelled UVI is much better for SAT relative to GB. By comparing CIMEL AOD measurements with measurements from other photometers we confirmed that they are accurate. As discussed later, the reason for the 10 - 20% underestimation of the UVI by the model is possibly that surface UV irradiance is strongly enhanced by clouds that are near 425 the solar disk during the day \(Fig. 5\).](#)

**Other factors of uncertainty in the modelling of the clear-sky UVI:** As [shown in Table 2](#)<sup>discussed earlier</sup>, fixed values of the [asymmetry parameter \(ASY\)](#), and the surface albedo have been used to derive the clear-sky UVI. The SSA has been

estimated using Kinne, (2019) climatology. Although ASY may deviate from the typical value of 0.7 depending on the type of aerosols, the uncertainties related to ASY are minor relative to the overall simulation uncertainties, as already discussed.

430 The fixed value of 0.05 for surface albedo is also not expected to induce uncertainties larger than 2% in the simulations (e.g., Fountoulakis et al., 2019). The standard correction (of 5%/km, i.e., ~8% for Davos) for the effect of altitude also induces small uncertainties (e.g. Blumthaler et al., 1997; Chubarova et al., 2016). By comparing the UVI simulated with UVSPEC with the results that were derived using the LUT (see Section 3.1.2), and then the correction for the effect of altitude, we found differences that were generally smaller than 1%, which shows that the uncertainties due to the combined effects of using the 435 LUT (i.e., interpolating through the dimensions of the LUT) and the post-correction for the effect of altitude are small. The horizon in Davos is limited by the tall mountains surrounding the site, which at SZAs larger than 75° can block the direct component of the solar irradiance, as well as a large fraction of the diffuse irradiance (Hülsen et al., 2020). Although we have not corrected the modelled UVI for the effect of limited horizon, for SZA<75°, this effect combined with the effect of default altitude correction was estimated to induce uncertainties smaller than 2%. Considering invariant atmospheric properties (i.e., 440 pressure and temperature profiles) based on a standard atmospheric profile (Anderson et al., 1986) which is not necessarily representative for a mountainous site such as Davos, introduces additional uncertainty, which however is expected to be minor relative to the overall uncertainty budget in our estimates. The used ETS and ozone absorption cross sections are more significant uncertainty factors (see Section 2.2).

### 3.1.2 All-skies UVI

445 For the default UVIOS2 setup the clear-sky UVI (that is derived using AOD from CAMS and TOC from TEMIS) is multiplied with the CMFUV to calculate the all-sky UVI. This method has been preferred instead of performing directly the simulations using cloud optical properties as libRadtran inputs because it is much faster and has a minor impact on the simulated UVI uncertainty compared to the uncertainty induced by the assumption of cloud homogeneity in the satellite pixel (e.g., Schenzer et al., 2023). The all-sky UVI that was calculated using the LUT, the all-sky UVI that was calculated directly 450 from libRadtran (for the altitude of the station and using cloud optical properties as inputs), and the UVI measured by QASUME are shown in Fig. 6-7 for DOY 188 - 191. During the cloudy DOYs 188 and 191 the variability in the modelled UVI (using both approaches) is in quite good agreement with the variability in the measured UVI. As shown in Fig. 78, both approaches result in correlation coefficients of ~ 0.95 between the measured and modelled UVIs. The differences between the measured and modelled UVIs (for SZAs below 75°) are presented in Fig. 89. For both modelling approaches the average 455 differences in the UVI are nearly identical (~ 0) with a nearly identical standard deviation (~ 1). From figures 6-7 and 87 - 9 it is obvious that the differences between the two modelling approaches are very small, and that the deviations originate mostly from the assumption of homogeneous distribution of clouds within the satellite pixel. The differences between the UVI from QASUME and the model (with both setups) are in some cases very large, reaching even values of ± 8. These large differences are mainly due to the model inability to predict accurately if the fraction of the solar disc that is occluded by clouds, especially 460 under broken cloud conditions.

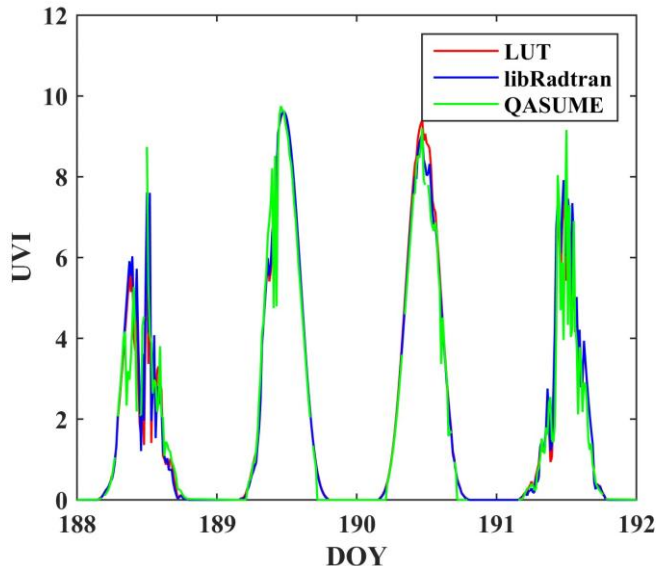


Figure 67. Measured UVI, and modelled UVI from the LUT and libRadtran.

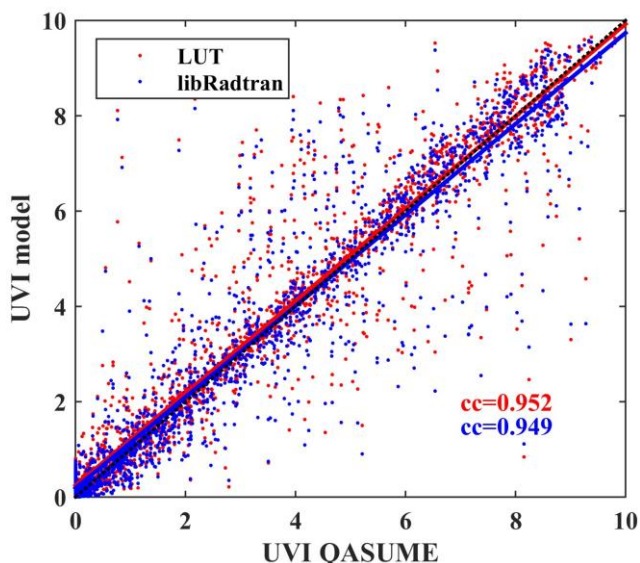
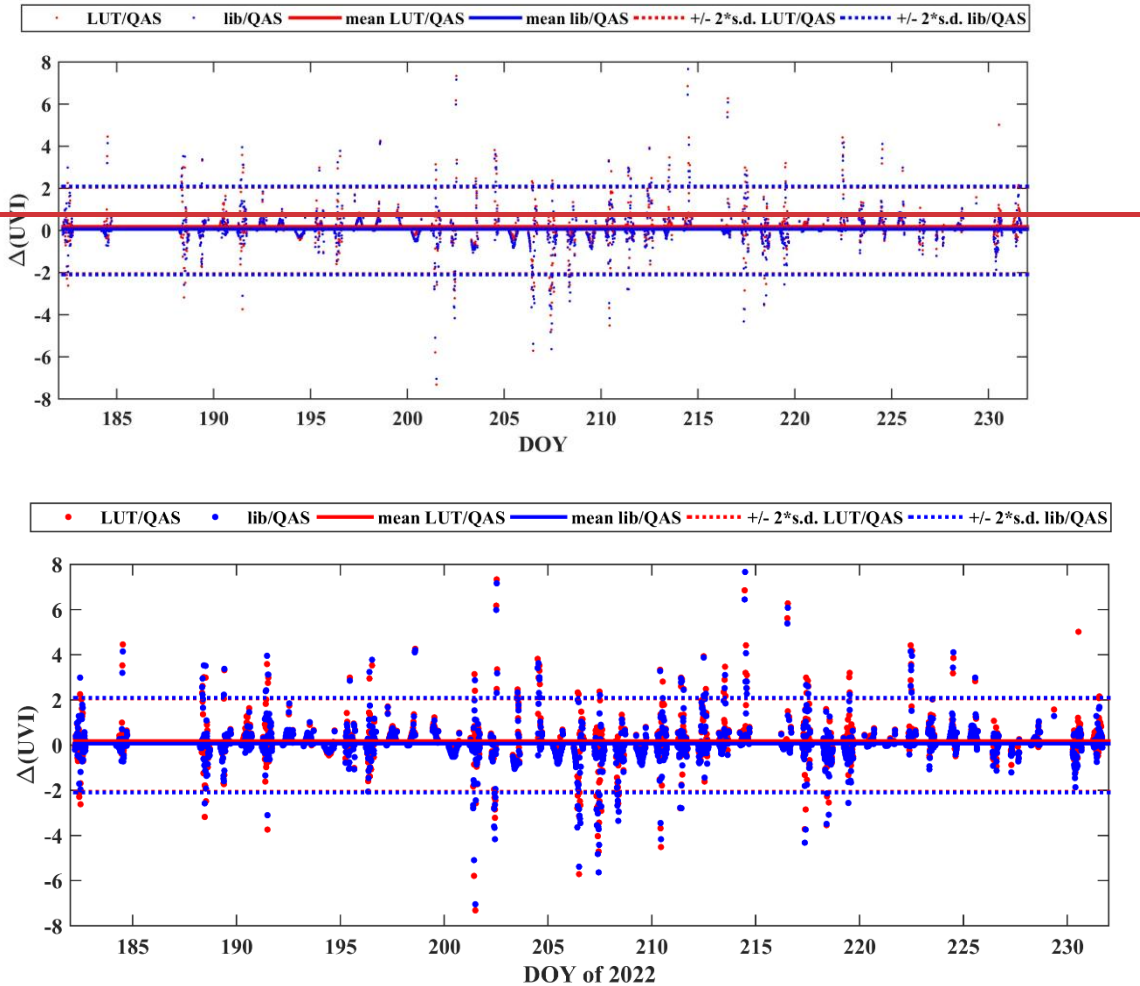


Figure 78. Correlation between measured UVI and UVI that was modelled using the two different approaches.



**Figure 89.** Differences (QASUME-model) between measured and modelled UVI

470 **3.2 Assessment of UVIOS2 for climatological studies**

In this section we assessed the accuracy of the modelled UVI when measured or reanalysis timeseries of AOD and TOC are used as inputs for the UVIOS2 system (instead of real time measurements or forecasts), that is the case when the system is used for climatological studies. The results of the comparison between the UVI from the QASUME and the UVI for the three different input datasets that were used as libRadtran inputs (i.e., ground-based TOC and AOD (GB), CAMS reanalysis AOD and TOC (CAMS), CAMS reanalysis AOD and OMI TOC (CAMS+OMI)) are shown in Fig. 910. The comparison has been performed again for  $\text{SZA} < 75^\circ$ . In all cases, the average agreement between the measured and the modelled UVI is nearly perfect (average differences of  $\sim 0$ ). The standard deviation ( $2 \times \text{standard deviation} \sim 1.9$ ) is very similar to the standard

475

deviation that was calculated for the UVI that was modelled using forecasted CAMS inputs. For the UVI that was modelled using GB data the standard deviation is slightly lower (2 x standard deviation  $\sim 1.7$ ).

480

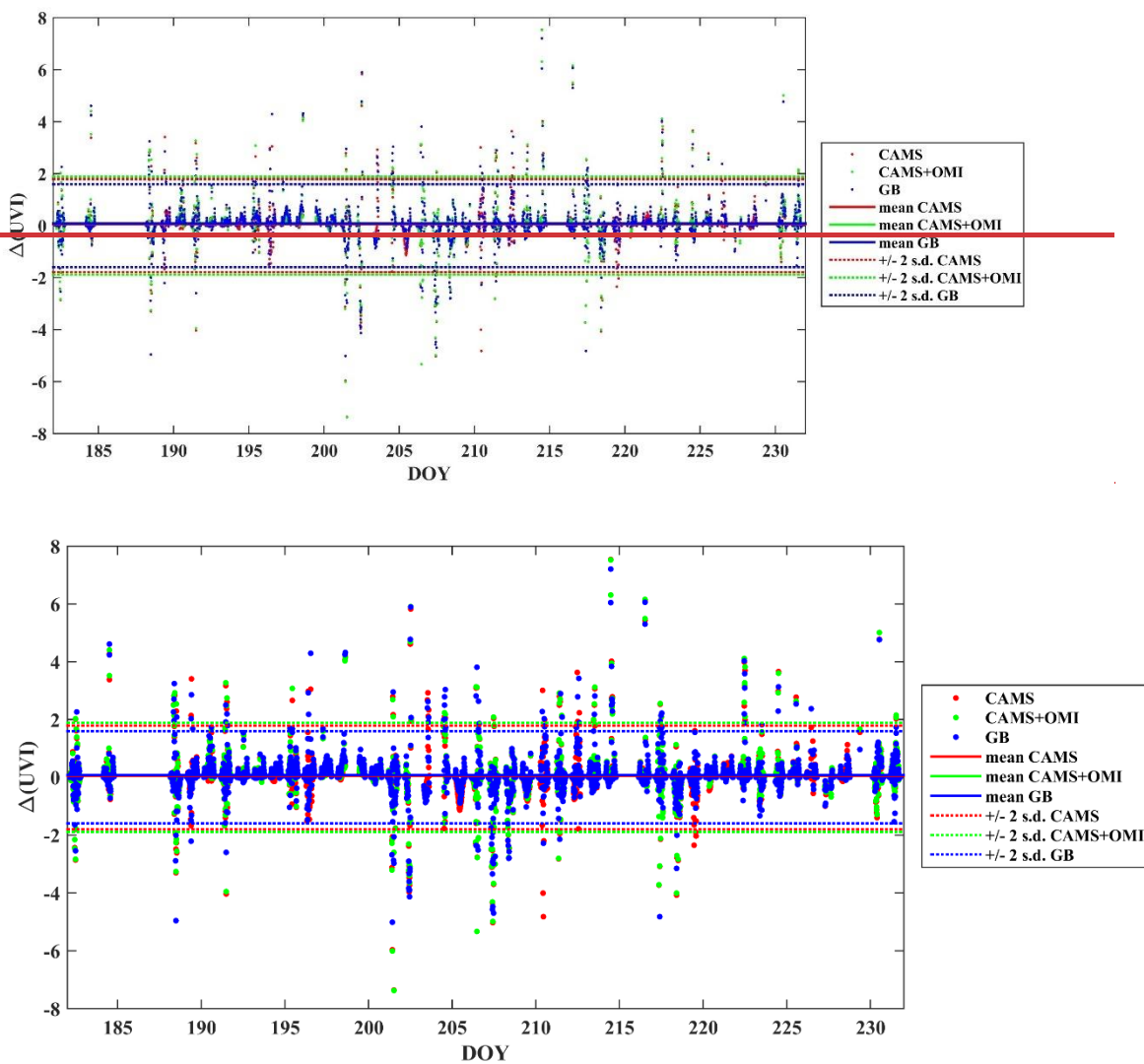


**Figure 910.** Differences between the measured UVI and the modelled UVI for different UVIOS2 inputs.

485

A summary of the results from the comparison between UVIOS2 and QASUME for the most uncertain (Nowcasting I - SAT) and the most accurate (Climatological III - GB) setup is presented in Table 34. The results for the two other setups (Climatological I – CAMS, Climatological II – CAMS+OMI) that were discussed earlier in the manuscript are very similar to those shown in Table 34, and thus they are not presented here.

**Table 3. Median differences and the corresponding standard deviation between UVIOS2 and QSUME for SZA < 75°.**

<u>Setup</u>	<u>All</u> <u>sky</u> <u>Δ(UVI)</u>	<u>St.</u> <u>d.</u>	<u>Clear</u> <u>sky</u> <u>Δ(UVI)</u>	<u>St.</u> <u>d.</u>	<u>All</u> <u>sky</u> <u>(%)</u>	<u>St.</u> <u>d.</u>	<u>Clear</u> <u>sky</u> <u>(%)</u>	<u>St. d.</u>
<u>Nowcasting_I</u> <u>(SAT)</u>	<u>-0.03</u>	<u>0.74</u>	<u>0.05</u>	<u>0.35</u>	<u>≤1%</u>	<u>66%</u>	<u>1.1%</u>	<u>6.2%</u>
<u>Nowcasting_II</u> <u>and</u> <u>Climatological</u> <u>III (GB)</u>	<u>-0.01</u>	<u>0.68</u>	<u>0.05</u>	<u>0.33</u>	<u>≤1%</u>	<u>63%</u>	<u>≤1%</u>	<u>5.5%</u>

490

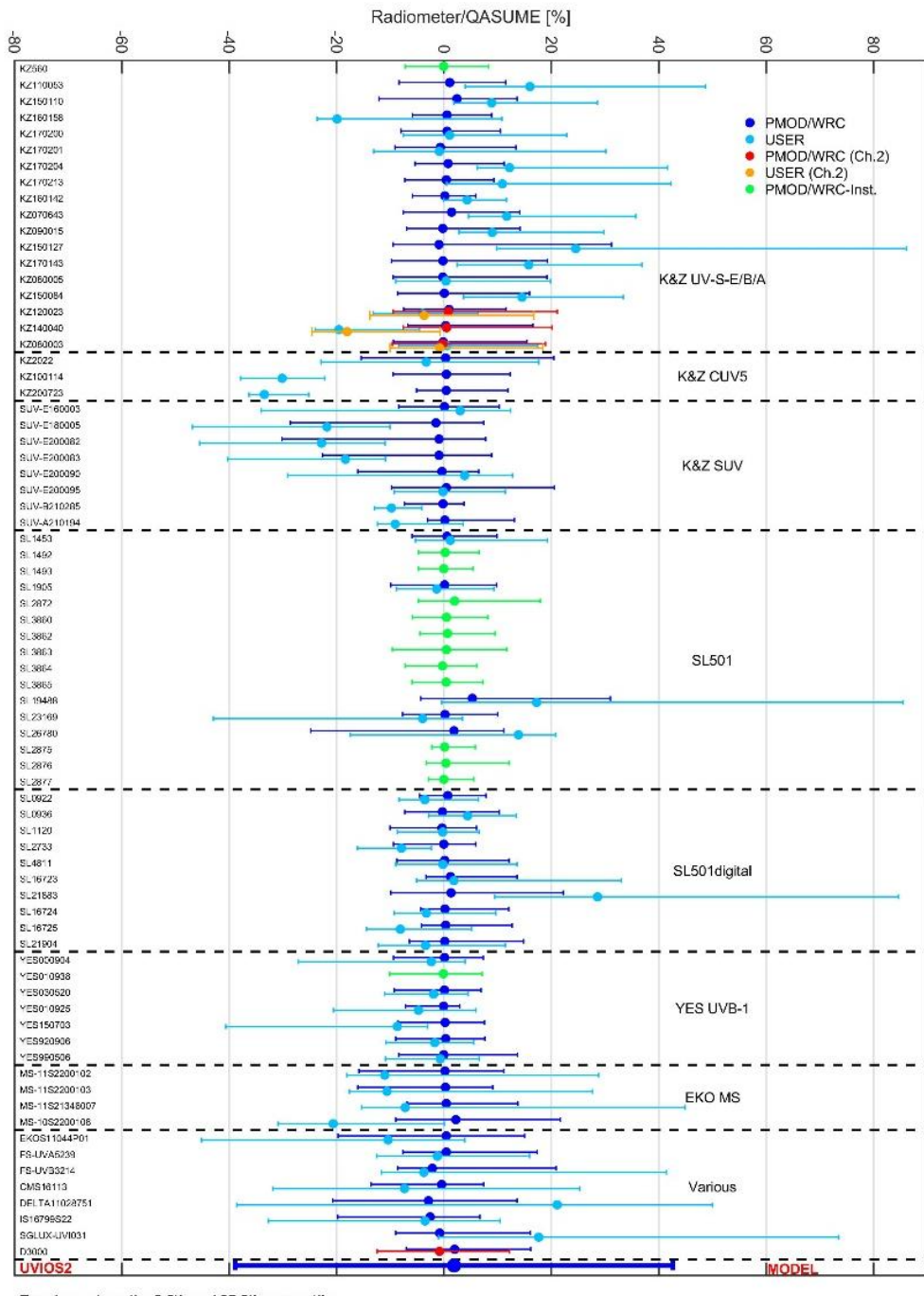
### 3.3 Comparison with the results of the campaign

In this section we tried to assess the performance of UVIOS2 (with the default setup, i.e., forecasted AOD and TOC from 495 CAMS and TEMIS respectively) with respect to the accuracy of the filter radiometers that participated to the campaign. The relative % differences between the UVI from the radiometers and QASUME (100% x (radiometer-QASUME)/QASUME) are presented for two cases: (1) when the calibration provided by the operator is used (USER) and (2) when the PMOD/WRC calibration is used (PMOD/WRC). In this section there is no extensive discussion relative to the results of the comparison between QASUME and the radiometers, since they have been already discussed thoroughly in Hülsen and Gröbner, (2023).

500 The median of differences between UVIs from QASUME and UVIOS2 is less than 2%, which confirms that UVIOS2 simulated very accurately the average UVI levels over Davos during the period of the campaign, as was also discussed in sections 3.1 and 3.2. Nevertheless, the 2.5<sup>th</sup> and 97.5<sup>th</sup> percentiles are at about -20% and 35% respectively. As shown in the previous sections this large spread is mostly due to the inability of the model to predict accurately the presence of clouds under broken cloud conditions.

505 When the USER calibration is used to derive the UVI from the radiometers, the range between the 2.5<sup>th</sup> - 97.5<sup>th</sup> percentile is in some cases of the order of 40%, and thus comparable to the corresponding range for UVIOS2 (~ 55%). When the PMOD/WRC calibration is used, the range between the 2.5<sup>th</sup> and 97.5<sup>th</sup> percentiles is in all cases below 20%. These latter findings show the significance of the systematic maintenance and calibration of the sensors.

510 From Fig. 11 it is clear that, although UVIOS2 achieves to simulate very accurately the average UVI levels, it is still significantly more uncertain than the measurements from usual UV radiometers when they are well calibrated and well maintained, especially under broken cloud conditions.



Errorbars show the 2.5th and 97.5th percentile.

**Figure 10.11** Relative (in %) difference between the UVI measured by QASUME and by the filter radiometers using the operator (USER) and the new (PMOD/WRC) calibration factors. Comparison has been also performed with the UVI from UVIOS2 ([SAT](#))

**configuration).** Displayed is the median of the ratio for the calibration period as well as the 2.5th and 97.5th percentile for each instrument (95% coverage). Figure has been originally published in (Hülsen and Gröbner, 2023).

## 4 Summary and conclusions

520 The UVIOS2 is an upgrade of the UVIOS system described in Kosmopoulos et al. (2021). We described the new features of the system, and evaluated in depth its performance at Davos, Switzerland during the UVCIII campaign. We assessed the accuracy of the UVIOS2 system when it is used for UVI forecasting and when it is used for climatological studies. To achieve that, the system outputs during the UVCIII campaign were compared to the measurements of the world reference QASUME, as well as to the measurements of the filter radiometers that participated to the campaign. The performance of the system was  
525 found to be excellent in simulating the average UVI levels, but uncertainties are larger in the simulations of the instantaneous UVI values. ~~A summary of the results from the comparison between UVIOS2 and QASUME for the most uncertain (Nowcasting I – SAT) and the most accurate (Climatological III – GB) setup is presented in Table 3. The results for the two other setups (Climatological I – CAMS, Climatological II – CAMS + OMI) that were discussed earlier in the manuscript are very similar to those shown in Table 3, and thus they are not presented here.~~

530 **Table 3. Median differences and the corresponding standard deviation between UVIOS2 and QSUME for SZA < 75°.**

Setup	All sky Δ(UVI)	St. d.	Clear sky Δ(UVI)	St. d.	All sky (%)	St. d.	Clear sky (%)	St. d.
<b>Nowcasting I (SAT)</b>	<b>-0.03</b>	<b>0.74</b>	<b>0.05</b>	<b>0.35</b>	<b>≤1%</b>	<b>66%</b>	<b>1.1%</b>	<b>6.2%</b>
<b>Nowcasting II and Climatological III (GB)</b>	<b>-0.01</b>	<b>0.68</b>	<b>0.05</b>	<b>0.33</b>	<b>≤1%</b>	<b>63%</b>	<b>1.1%</b>	<b>5.5%</b>

Our analysis ~~shows~~ showed that the parameterization used to derive CMFUV works quite well and has reduced processing time significantly without affecting the accuracy in the system outputs. This is in agreement with the findings of Papachristopoulou et al. (2024) who have shown that the parameterization used to derive the CMF (for total solar irradiance) 535 from COT works well. Further investigation is needed to assess the uncertainties due to the cloud effect parameterization over higher albedo terrains, although we expect that the assumption of homogeneity in the satellite pixel would still be the main uncertainty factor (e.g., large gradients in cloudiness, aerosol properties, surface albedo, surface altitude).

The satellite algorithm considers that each pixel is homogeneously covered by clouds, and thus it cannot accurately determine under inhomogeneous cloudiness conditions whether the solar disc is occluded or unoccluded. Furthermore, when solar disc 540 is occluded, ~~we do not know the exact there are uncertainties in the retrieved COT, and even larger uncertainties in the CMFUV~~

that is subsequently calculated. The above can result in very large (especially %) differences between the measurements and the simulations. When the sun is unoccluded, broken clouds near the solar disc in the sky can contribute to the enhancement enhance of the UVI at the surface significantly, by up to 20% according to our findings.

The differences between the measured, forecasted, and reanalysis AOD and TOC that were used as inputs are not critical for 545 the accuracy of the UVIOS2 outputs for Davos, and thus the performance of UVIOS2 does not differ significantly when it is used as a forecasting tool or as a tool for climatological studies. Under cloudless conditions the role of SSA was found to be equally important to the role of AOD, even at a (usually) low aerosol mountainous site such as Davos.

~~The uncertainty in the UVIOS2 forecasts was found to be comparable to the measurements of filter radiometers when they were not properly calibrated, but 3 times larger compared to the measurements of accurately calibrated radiometers, which shows the significance of systematic and accurate calibration of such instruments.~~

The differences between measured and modelled UVI have been also discussed in previous studies (e.g., ~~(De Backer et al., 2001; Fioletov et al., 2004; Kylling et al., 1997; Mayer et al., 1997; Reuder and Schwander, 1999; Weihs and Webb, 1997)~~), which have also shown that the assumptions relative to the aerosol optical properties constitute a major uncertainty factor under cloudless sky conditions. Uncertainties of 5–8% at 380 nm and even larger at 305 nm were associated ~~to-with~~ the 555 assumptions related to the aerosol optical properties. The significant role of clouds in the UVI forecasting has been also discussed in Malinovic-Milicevic and Mihailovic (2011), who used a numerical model to estimate the UVI at Vojvodina region (Serbia). Vitt et al. (2020) constructed UVI maps for whole Europe based on monthly means and showed that uncertainties in surface albedo can be also significant over mountainous mid-latitude sites in winter. Dahlback and Stamnes (1991) reported that at the Tibetan Plateau (3000–5000 m a.s.l.) the UVI can be enhanced by ~30% under broken cloud conditions compared 560 to cloudless sky conditions. Similar impacts by clouds on the UVI were reported by Allaart et al. (2004).

Our study makes clear that there is a need for more accurate representation of the SSA in UV models in order to achieve more accurate modelling under cloudless conditions, even for low aerosol sites such as Davos. When AOD is 0.3 – 0.4, the effect of changes in the AOD is similar with the effect of changes of the same magnitude in the SSA. SSA measurements at shorter, and more effective regarding their biological impacts, UV wavelengths are not easy to perform, and long-time series are not 565 available ~~(e.g.,~~ (e.g., Bais et al., 2019; Corr et al., 2009; Go et al., 2020; Mok et al., 2016, 2018). Capturing the instantaneous impact of clouds using satellite images is challenging, especially for enhancement events. In this study we showed that enhancement events can not be easily captured even when ground-based information is used. Since using satellite-based cloud information is the only way to forecast the UVI at large spatial scales, the accuracy in the description of the effects of clouds is a common problem for UV models that cannot be easily solved.

## 570 Acknowledgments

This work was supported by computational time granted by the National Infrastructures for Research and Technology S.A. (GRNET) at the National HPC facility – ARIS – under project ID pa210301-SO-LISIS. The European Commission project

“EXCELSIOR”: ERATOSTHENES: Excellence Research Centre for Earth Surveillance and Space-Based Monitoring of the Environment (grant no. 857510) is also acknowledged. C. S. Zerefos would like to acknowledge CAMS2\_82 Project: 575 Evaluation and Quality Control (EQC) of global products. D. Kouklaki would like to acknowledge the PANGEA4CalVal project (Grant Agreement 101079201) funded by the European Union.

S. Kazadzis acknowledges ACTRIS-CH (Aerosol, Clouds and Trace Gases Research Infrastructure – Swiss contribution), funded by the State Secretariat for Education, Research and Innovation. SK, IF, KP would like to acknowledge HARMONIA (International network for harmonization of atmospheric aerosol retrievals from ground-based photometers; grant no. 580 CA21119), supported by COST (European Cooperation in Science and Technology).

## Financial Support

This project has received funding from the European Union's Horizon 2020 research and innovation programme EIFFEL under grant agreement No 101003518. This work has been funded by the COST Action HARMONIA, CA21119, supported by COST (European Cooperation in Science and Technology).

## 585 Code and Data availability

Analytical description and instructions on how to access the model are provided in Kosmopoulos et al., (2021). All codes and datasets that are necessary to reproduce the results used in this paper are archived on Zenodo (Fountoulakis, 2024).

## Competing interests

The contact author has declared that none of the authors has any competing interests.

## 590 Author contribution

Conceptualization: SK, IF. Methodology: SK, IF and KP. Formal analysis: IF, KP, JG, GH, and DK. Software: IF, KP, and I-PR. Validation: IF, KP, SK, GH, and JG. Investigation: IF and KP. Resources: SK and CK. Data curation: IF, KP, NK, JG and GH. Visualization: IF, KP and GH. Writing (original draft preparation): IF, KP, and AM. Supervision: SK. Writing (review and editing): IF, KP, SK, JG, GH, I-PR, DK, AM, CK, and CZ. All authors gave final approval for publication.

## References

Allaart, M., van Weele, M., Fortuin, P., and Kelder, H.: An empirical model to predict the UV-index based on solar zenith angles and total ozone, *Meteorological Applications*, 11, 59–65, <https://doi.org/10.1017/S1350482703001130>, 2004.

Anderson, G., Clough, S., Kneizys, F., Chetwynd, J., and Shettle, E.: AFGL Atmospheric Constituent Profiles (0.120km), 46, 600 1986.

Armstrong, B. K. and Cust, A. E.: Sun exposure and skin cancer, and the puzzle of cutaneous melanoma: A perspective on Fears et al. Mathematical models of age and ultraviolet effects on the incidence of skin cancer among whites in the United States. *American Journal of Epidemiology* 1977; , *Cancer Epidemiol*, 48, 147–156, <https://doi.org/https://doi.org/10.1016/j.canep.2017.04.004>, 2017.

Arola, A., Kalliskota, S., den Outer, P. N., Edvardsen, K., Hansen, G., Koskela, T., Martin, T. J., Matthijsen, J., Meerkoetter, R., Peeters, P., Seckmeyer, G., Simon, P. C., Slaper, H., Taalas, P., and Verdebout, J.: Assessment of four methods to estimate surface UV radiation using satellite data, by comparison with ground measurements from four stations in Europe, *Journal of Geophysical Research: Atmospheres*, 107, ACL 11-1-ACL 11-11, <https://doi.org/https://doi.org/10.1029/2001JD000462>, 2002.

Arola, A., Wandji Nyamsi, W., Lipponen, A., Kazadzis, S., Krotkov, N. A., and Tamminen, J.: Rethinking the correction for absorbing aerosols in the OMI- and TROPOMI-like surface UV algorithms, *Atmos. Meas. Tech.*, 14, 4947–4957, <https://doi.org/10.5194/amt-14-4947-2021>, 2021.

De Backer, H., Koepke, P., Bais, A., de Cabo, X., Frei, T., Gillotay, D., Haite, C., Heikkilä, A., Kazantzidis, A., Koskela, T., Kyrö, E., Lapeta, B., Lorente, J., Masson, K., Mayer, B., Plets, H., Redondas, A., Renaud, A., Schaubberger, G., Schmalwieser, A., Schwander, H., and Vanicek, K.: Comparison of measured and modelled uv indices for the assessment of health risks, *Meteorological Applications*, 8, 267–277, <https://doi.org/10.1017/S1350482701003024>, 2001.

Bais, A. F., Gardiner, B. G., Slaper, H., Blumthaler, M., Bernhard, G., McKenzie, R., Webb, A. R., Seckmeyer, G., Kjeldstad, B., Koskela, T., Kirsch, P. J., Gröbner, J., Kerr, J. B., Kazadzis, S., Leszczynski, K., Wardle, D., Josefsson, W., Brogniez, C., Gillotay, D., Reinen, H., Weihs, P., Svenoe, T., Eriksen, P., Kuik, F., and Redondas, A.: SUSPEN intercomparison of ultraviolet spectroradiometers, *Journal of Geophysical Research: Atmospheres*, 106, 12509–12525, <https://doi.org/https://doi.org/10.1029/2000JD900561>, 2001.

Bais, A. F., Bernhard, G., McKenzie, R. L., Aucamp, P. J., Young, P. J., Ilyas, M., Jöckel, P., and Deushi, M.: Ozone–climate interactions and effects on solar ultraviolet radiation, *Photochemical & Photobiological Sciences*, 18, 602–640, <https://doi.org/10.1039/C8PP90059K>, 2019.

Bernhard, G., Booth, C. R., and Ehramjan, J. C.: Comparison of UV irradiance measurements at Summit, Greenland; Barrow, Alaska; and South Pole, Antarctica, *Atmos Chem Phys*, 8, 4799–4810, <https://doi.org/10.5194/acp-8-4799-2008>, 2008.

Bernhard, G., Arola, A., Dahlback, A., Fioletov, V., Heikkilä, A., Johnsen, B., Koskela, T., Lakkala, K., Svendby, T., and Tamminen, J.: Comparison of OMI UV observations with ground-based measurements at high northern latitudes, *Atmos. Chem. Phys.*, 15, 7391–7412, <https://doi.org/10.5194/acp-15-7391-2015>, 2015.

630 Bernhard, G. H., Bais, A. F., Aucamp, P. J., Klekociuk, A. R., Liley, J. B., and McKenzie, R. L.: Stratospheric ozone, UV radiation, and climate interactions, *Photochemical & Photobiological Sciences*, 22, 937–989, <https://doi.org/10.1007/s43630-023-00371-y>, 2023.

Blumthaler, M.: UV Monitoring for Public Health, <https://doi.org/10.3390/ijerph15081723>, 2018.

Blumthaler, M., Webb, A. R., Seckmeyer, G., Bais, A. F., Huber, M., and Mayer, B.: Simultaneous spectroradiometry: A study of solar UV irradiance at two altitudes, *Geophys Res Lett*, 21, 2805–2808, <https://doi.org/10.1029/94GL02786>, 1994.

635 Blumthaler, M., Salzgeber, M., and Ambach, W.: OZONE AND ULTRAVIOLET-B IRRADIANCES: EXPERIMENTAL DETERMINATION OF THE RADIATION AMPLIFICATION FACTOR, *Photochem Photobiol*, 61, 159–162, <https://doi.org/10.1111/j.1751-1097.1995.tb03954.x>, 1995.

Blumthaler, M., Ambach, W., and Ellinger, R.: Increase in solar UV radiation with altitude, *J Photochem Photobiol B*, 39, 640 130–134, [https://doi.org/10.1016/S1011-1344\(96\)00018-8](https://doi.org/10.1016/S1011-1344(96)00018-8), 1997.

Brogniez, C., Auriol, F., Deroo, C., Arola, A., Kujanpää, J., Sauvage, B., Kalakoski, N., Pitkänen, M. R. A., Catalfamo, M., Metzger, J.-M., Tournois, G., and Da Conceicao, P.: Validation of satellite-based noontime UVI with NDACC ground-based instruments: influence of topography, environment and satellite overpass time, *Atmos Chem Phys*, 16, 15049–15074, <https://doi.org/10.5194/acp-16-15049-2016>, 2016.

645 Caldwell, M. M., Björn, L. O., Bornman, J. F., Flint, S. D., Kulandaivelu, G., Teramura, A. H., and Tevini, M.: Effects of increased solar ultraviolet radiation on terrestrial ecosystems, *J Photochem Photobiol B*, 46, 40–52, [https://doi.org/https://doi.org/10.1016/S1011-1344\(98\)00184-5](https://doi.org/https://doi.org/10.1016/S1011-1344(98)00184-5), 1998.

Carlund, T., Kouremeti, N., Kazadzis, S., and Gröbner, J.: Aerosol optical depth determination in the UV using a four-channel precision filter radiometer, *Atmos Meas Tech*, 10, 905–923, <https://doi.org/10.5194/amt-10-905-2017>, 2017.

650 Casale, G. R., Siani, A. M., Diémoz, H., Agnesod, G., Parisi, A. V., and Colosimo, A.: Extreme UV index and solar exposures at Plateau Rosà (3500 m a.s.l.) in Valle d’Aosta Region, Italy, *Science of The Total Environment*, 512–513, 622–630, <https://doi.org/10.1016/j.scitotenv.2015.01.049>, 2015.

Chubarova, N. and Zhdanova, Y.: The assessment of UV resources over Northern Eurasia, 764–767, <https://doi.org/10.1063/1.4804882>, 2013.

655 Chubarova, N., Zhdanova, Y., and Nezval, Y.: A new parameterization of the UV irradiance altitude dependence for clear-sky conditions and its application in the on-line UV tool over Northern Eurasia, *Atmos Chem Phys*, 16, 11867–11881, <https://doi.org/10.5194/acp-16-11867-2016>, 2016.

Corr, C. A., Krotkov, N., Madronich, S., Slusser, J. R., Holben, B., Gao, W., Flynn, J., Lefer, B., and Kreidenweis, S. M.: Retrieval of aerosol single scattering albedo at ultraviolet wavelengths at the T1 site during MILAGRO, *Atmos Chem Phys*, 660 9, 5813–5827, <https://doi.org/10.5194/acp-9-5813-2009>, 2009.

Dahlback, A. and Stamnes, K.: A new spherical model for computing the radiation field available for photolysis and heating at twilight, *Planet Space Sci*, 39, 671–683, [https://doi.org/https://doi.org/10.1016/0032-0633\(91\)90061-E](https://doi.org/10.1016/0032-0633(91)90061-E), 1991.

Dahlback, A., Gelsor, N., Stamnes, J. J., and Gjessing, Y.: UV measurements in the 3000–5000 m altitude region in Tibet, *Journal of Geophysical Research: Atmospheres*, 112, <https://doi.org/10.1029/2006JD007700>, 2007.

665 Deneke, H., Barrientos-Velasco, C., Bley, S., Hünerbein, A., Lenk, S., Macke, A., Meirink, J. F., Schroedter-Homscheidt, M., Senf, F., Wang, P., Werner, F., and Wittuhn, J.: Increasing the spatial resolution of cloud property retrievals from Meteosat SEVIRI by use of its high-resolution visible channel: implementation and examples, *Atmos Meas Tech*, 14, 5107–5126, <https://doi.org/10.5194/amt-14-5107-2021>, 2021.

Derrien, M. and Le Gléau, H.: MSG/SEVIRI cloud mask and type from SAFNWC, *Int J Remote Sens*, 26, 4707–4732, 670 <https://doi.org/10.1080/01431160500166128>, 2005.

Diffey, B. L.: Solar ultraviolet radiation effects on biological systems, *Phys Med Biol*, 36, 299–328, <https://doi.org/10.1088/0031-9155/36/3/001>, 1991.

van Dijk, A., Slaper, H., den Outer, P. N., Morgenstern, O., Braesicke, P., Pyle, J. A., Garny, H., Stenke, A., Dameris, M., Kazantzidis, A., Tourpali, K., and Bais, A. F.: Skin cancer risks avoided by the Montreal Protocol--worldwide 675 modeling integrating coupled climate-chemistry models with a risk model for UV., *Photochem Photobiol*, 89, 234–246, <https://doi.org/10.1111/j.1751-1097.2012.01223.x>, 2013.

Dürr, B., and R. Philipona, Automatic cloud amount detection by surface longwave downward radiation measurements, *J. Geophys. Res.*, 109, D05201, doi:10.1029/2003JD004182, 2004.

Dvorkin, A. Y. and Steinberger, E. H.: MODELING THE ALTITUDE EFFECT ON SOLAR UV RADIATION, *Solar Energy*, 680 65, 181–187, [https://doi.org/10.1016/S0038-092X\(98\)00126-1](https://doi.org/10.1016/S0038-092X(98)00126-1), 1999.

Egli, L., Gröbner, J., Hülsen, G., Bachmann, L., Blumthaler, M., Dubard, J., Khazova, M., Kift, R., Hoogendijk, K., Serrano, A., Smedley, A., and Vilaplana, J.-M.: Quality assessment of solar UV irradiance measured with array spectroradiometers, *Atmos. Meas. Tech.*, 9, 1553–1567, <https://doi.org/10.5194/amt-9-1553-2016>, 2016.

Emde, C., Buras-Schnell, R., Kylling, A., Mayer, B., Gasteiger, J., Hamann, U., Kylling, J., Richter, B., Pause, C., Dowling, 685 T., and Bugliaro, L.: The libRadtran software package for radiative transfer calculations (version 2.0.1), *Geosci. Model Dev.*, 9, 1647–1672, <https://doi.org/10.5194/gmd-9-1647-2016>, 2016.

Erickson III, D. J., Sulzberger, B., Zepp, R. G., and Austin, A. T.: Effects of stratospheric ozone depletion, solar UV radiation, and climate change on biogeochemical cycling: interactions and feedbacks, *Photochemical & Photobiological Sciences*, 14, 127–148, <https://doi.org/10.1039/C4PP90036G>, 2015.

690 Feister, U. and Grewe, R.: SPECTRAL ALBEDO MEASUREMENTS IN THE UV and VISIBLE REGION OVER DIFFERENT TYPES OF SURFACES, *Photochem Photobiol*, 62, 736–744, <https://doi.org/https://doi.org/10.1111/j.1751-1097.1995.tb08723.x>, 1995.

Feister, U., Laschewski, G., and Grewe, R.-D.: UV index forecasts and measurements of health-effective radiation, *J Photochem Photobiol B*, 102, 55–68, <https://doi.org/https://doi.org/10.1016/j.jphotobiol.2010.09.005>, 2011.

695 Fioletov, V. E., Kimlin, M. G., Krotkov, N., McArthur, L. J. B., Kerr, J. B., Wardle, D. I., Herman, J. R., Meltzer, R., Mathews, T. W., and Kaurola, J.: UV index climatology over the United States and Canada from ground-based and satellite estimates, *Journal of Geophysical Research: Atmospheres*, 109, <https://doi.org/10.1029/2004JD004820>, 2004.

Fountoulakis, I.: Data and code for “Assessment of the accuracy in UV index modelling using the UVIOS2 system during the UVC-III campaign,” <https://doi.org/10.5281/zenodo.14237637>, November 2024.

700 Fountoulakis, I., Siomos, N., Natsi, A., Drosoglou, T., and Bais, A. F.: Deriving Aerosol Absorption Properties from Solar Ultraviolet Radiation Spectral Measurements at Thessaloniki, Greece, <https://doi.org/10.3390/rs11182179>, 2019.

Fountoulakis, I., Diémoz, H., Siani, A. M., Hülsen, G., and Gröbner, J.: Monitoring of solar spectral ultraviolet irradiance in Aosta, Italy, *Earth Syst Sci Data*, 12, 2787–2810, <https://doi.org/10.5194/essd-12-2787-2020>, 2020a.

Fountoulakis, I., Diémoz, H., Siani, A.-M., Laschewski, G., Filippa, G., Arola, A., Bais, A. F., De Backer, H., Lakkala, K., 705 Webb, A. R., De Bock, V., Karppinen, T., Garane, K., Kapsomenakis, J., Koukouli, M.-E., and Zerefos, C. S.: Solar UV Irradiance in a Changing Climate: Trends in Europe and the Significance of Spectral Monitoring in Italy, <https://doi.org/10.3390/environments7010001>, 2020b.

Fragkos, K., Bais, A. F., Balis, D., Meleti, C., and Koukouli, M. E.: The Effect of Three Different Absorption Cross-Sections and their Temperature Dependence on Total Ozone Measured by a Mid-Latitude Brewer Spectrophotometer, *Atmosphere-Ocean*, 53, 19–28, <https://doi.org/10.1080/07055900.2013.847816>, 2015.

710 Fragkos, K., Fountoulakis, I., Charalampous, G., Papachristopoulou, K., Nisantzi, A., Hadjimitsis, D., and Kazadzis, S.: Twenty-Year Climatology of Solar UV and PAR in Cyprus: Integrating Satellite Earth Observations with Radiative Transfer Modeling, *Remote Sens (Basel)*, 16, <https://doi.org/10.3390/rs16111878>, 2024.

Fu, Q.: An Accurate Parameterization of the Solar Radiative Properties of Cirrus Clouds for Climate Models, *J Clim*, 9, 2058–2082, [https://doi.org/10.1175/1520-0442\(1996\)009<2058:AAPOTS>2.0.CO;2](https://doi.org/10.1175/1520-0442(1996)009<2058:AAPOTS>2.0.CO;2), 1996.

715 Fu, Q., Yang, P., and Sun, W. B.: An Accurate Parameterization of the Infrared Radiative Properties of Cirrus Clouds for Climate Models, *J Clim*, 11, 2223–2237, [https://doi.org/10.1175/1520-0442\(1998\)011<2223:AAPOTI>2.0.CO;2](https://doi.org/10.1175/1520-0442(1998)011<2223:AAPOTI>2.0.CO;2), 1998.

Garane, K., Bais, A. F., Kazadzis, S., Kazantzidis, A., and Meleti, C.: Monitoring of UV spectral irradiance at Thessaloniki (1990–2005): data re-evaluation and quality control, *Ann. Geophys.*, 24, 3215–3228, <https://doi.org/10.5194/angeo-24-3215-2006>, 2006.

720 Giles, D. M., Sinyuk, A., Sorokin, M. G., Schafer, J. S., Smirnov, A., Slutsker, I., Eck, T. F., Holben, B. N., Lewis, J. R., Campbell, J. R., Welton, E. J., Korkin, S. V., and Lyapustin, A. I.: Advancements in the Aerosol Robotic Network (AERONET) Version 3 database – automated near-real-time quality control algorithm with improved cloud screening for Sun photometer aerosol optical depth (AOD) measurements, *Atmos Meas Tech*, 12, 169–209, <https://doi.org/10.5194/amt-12-169-2019>, 2019.

725 Go, S., Kim, J., Mok, J., Irie, H., Yoon, J., Torres, O., Krotkov, N. A., Labow, G., Kim, M., Koo, J.-H., Choi, M., and Lim, H.: Ground-based retrievals of aerosol column absorption in the UV spectral region and their implications for GEMS measurements, *Remote Sens Environ*, 245, 111759, <https://doi.org/10.1016/j.rse.2020.111759>, 2020.

Gröbner, J. and Sperfeld, P.: Direct traceability of the portable QASUME irradiance scale to the primary irradiance standard  
730 of the PTB, *Metrologia*, 42, 134–139, <https://doi.org/10.1088/0026-1394/42/2/008>, 2005.

Gröbner, J., Schreder, J., Kazadzis, S., Bais, A. F., Blumthaler, M., Görts, P., Tax, R., Koskela, T., Seckmeyer, G., Webb, A. R., and Rembges, D.: Traveling reference spectroradiometer for routine quality assurance of spectral solar ultraviolet irradiance measurements, *Appl Opt*, 44, 5321–5331, <https://doi.org/10.1364/AO.44.005321>, 2005.

Gröbner, J., Blumthaler, M., Kazadzis, S., Bais, A., Webb, A., Schreder, J., Seckmeyer, G., and Rembges, D.: Quality  
735 assurance of spectral solar UV measurements: results from 25 UV monitoring sites in Europe, 2002 to 2004, *Metrologia*, 43, S66–S71, <https://doi.org/10.1088/0026-1394/43/2/s14>, 2006.

Gröbner, J., Kröger, I., Egli, L., Hülsen, G., Riechelmann, S., and Sperfeld, P.: The high-resolution extraterrestrial solar spectrum (QASUMEFTS) determined from ground-based solar irradiance measurements, *Atmos Meas Tech*, 10, 3375–3383, <https://doi.org/10.5194/amt-10-3375-2017>, 2017.

740 Gröbner, J., Schill, H., Egli, L., and Stübi, R.: Consistency of total column ozone measurements between the Brewer and Dobson spectroradiometers of the LKO Arosa and PMOD/WRC Davos, *Atmos Meas Tech*, 14, 3319–3331, <https://doi.org/10.5194/amt-14-3319-2021>, 2021.

Häder, D.-P.: Effects of enhanced solar ultraviolet radiation on aquatic ecosystems, in: *Biophysics of photoreceptors and photomovements in microorganisms*, Springer, 157–172, 1991.

745 Häder, D.-P., Kumar, H. D., Smith, R. C., and Worrest, R. C.: Effects on aquatic ecosystems, *J Photochem Photobiol B*, 46, 53–68, [https://doi.org/https://doi.org/10.1016/S1011-1344\(98\)00185-7](https://doi.org/10.1016/S1011-1344(98)00185-7), 1998.

Herman, J. R., Krotkov, N., Celarier, E., Larko, D., and Labow, G.: Distribution of UV radiation at the Earth's surface from TOMS-measured UV-backscattered radiances, *Journal of Geophysical Research: Atmospheres*, 104, 12059–12076, [https://doi.org/https://doi.org/10.1029/1999JD900062](https://doi.org/10.1029/1999JD900062), 1999.

750 Hoffmann, G. and Meffert, H.: Apparent contradiction between negative effects of UV radiation and positive effects of sun exposure., *Ger Med Sci*, 3, Doc01, 2005.

Holben, B. N., Eck, T. F., Slutsker, I., Tanré, D., Buis, J. P., Setzer, A., Vermote, E., Reagan, J. A., Kaufman, Y. J., Nakajima, T., Lavenu, F., Jankowiak, I., and Smirnov, A.: AERONET—A Federated Instrument Network and Data Archive for Aerosol Characterization, *Remote Sens Environ*, 66, 1–16, [https://doi.org/https://doi.org/10.1016/S0034-4257\(98\)00031-5](https://doi.org/10.1016/S0034-4257(98)00031-5), 1998.

755 Hu, Y. X. and Stamnes, K.: An Accurate Parameterization of the Radiative Properties of Water Clouds Suitable for Use in Climate Models, *J Clim*, 6, 728–742, [https://doi.org/10.1175/1520-0442\(1993\)006<0728:AAPOTR>2.0.CO;2](https://doi.org/10.1175/1520-0442(1993)006<0728:AAPOTR>2.0.CO;2), 1993.

Hülsen, G. and Gröbner, J.: Characterization and calibration of ultraviolet broadband radiometers measuring erythemally weighted irradiance, *Appl Opt*, 46, 5877–5886, <https://doi.org/10.1364/AO.46.005877>, 2007.

Hülsen, G. and Gröbner, J.: Report of the Third International Solar UV Radiometer Calibration Campaign (UVC-III), GAW  
760 report No 284, <https://library.wmo.int/idurl/4/68642>, 2023.

Hülsen, G., Gröbner, J., Nevas, S., Sperfeld, P., Egli, L., Porrovecchio, G., and Smid, M.: Traceability of solar UV measurements using the Qasume reference spectroradiometer., *Appl Opt*, 55, 7265–7275, <https://doi.org/10.1364/AO.55.007265>, 2016.

Hülsen, G., Gröbner, J., Bais, A., Blumthaler, M., Diémoz, H., Bolsée, D., Diaz, A., Fountoulakis, I., Naranen, E., Schreder, J., Stefania, F., and Guerrero, J. M. V.: Second solar ultraviolet radiometer comparison campaign {UVC}-{II}, *Metrologia*, 57, 35001, <https://doi.org/10.1088/1681-7575/ab74e5>, 2020.

Inness, A., Ades, M., Agustí-Panareda, A., Barr, J., Benedictow, A., Blechschmidt, A. M., Jose Dominguez, J., Engelen, R., Eskes, H., Flemming, J., Huijnen, V., Jones, L., Kipling, Z., Massart, S., Parrington, M., Peuch, V. H., Razinger, M., Remy, S., Schulz, M., and Suttie, M.: The CAMS reanalysis of atmospheric composition, *Atmos Chem Phys*, 19, 3515–3556, <https://doi.org/10.5194/acp-19-3515-2019>, 2019.

Juzeniene, A. and Moan, J.: Beneficial effects of UV radiation other than via vitamin D production, *Dermatoendocrinol*, 4, 109–117, <https://doi.org/10.4161/derm.20013>, 2012.

Juzeniene, A., Brekke, P., Dahlback, A., Andersson-Engels, S., Reichrath, J., Moan, K., Holick, M. F., Grant, W. B., and Moan, J.: Solar radiation and human health, *Reports on Progress in Physics*, 74, 66701, <https://doi.org/10.1088/0034-4885/74/6/066701>, 2011.

Kazadzis, S., Bais, A., Arola, A., Krotkov, N., Kouremeti, N., and Meleti, C.: Ozone Monitoring Instrument spectral UV irradiance products: comparison with ground based measurements at an urban environment, *Atmos. Chem. Phys.*, 9, 585–594, <https://doi.org/10.5194/acp-9-585-2009>, 2009.

Kazadzis, S., Raptis, P., Kouremeti, N., Amiridis, V., Arola, A., Gerasopoulos, E., and Schuster, G. L.: Aerosol absorption retrieval at ultraviolet wavelengths in a complex environment, *Atmos. Meas. Tech.*, 9, 5997–6011, <https://doi.org/10.5194/amt-9-5997-2016>, 2016.

Kerr, J. B.: The Brewer Spectrophotometer BT - UV Radiation in Global Climate Change: Measurements, Modeling and Effects on Ecosystems, edited by: Gao, W., Slusser, J. R., and Schmoldt, D. L., Springer Berlin Heidelberg, Berlin, Heidelberg, 160–191, [https://doi.org/10.1007/978-3-642-03313-1\\_6](https://doi.org/10.1007/978-3-642-03313-1_6), 2010.

Kerr, J. B., McElroy, C. T., Wardle, D. I., Olafson, R. A., and Evans, W. F. J.: The Automated Brewer Spectrophotometer BT - Atmospheric Ozone, 396–401, 1985.

Khatri, P., Takamura, T., Nakajima, T., Estellés, V., Irie, H., Kuze, H., Campanelli, M., Sinyuk, A., Lee, S. -M., Sohn, B. J., Pandithurai, G., Kim, S. -W., Yoon, S. C., Martinez-Lozano, J. A., Hashimoto, M., Devara, P. C. S., and Manago, N.: Factors for inconsistent aerosol single scattering albedo between SKYNET and AERONET, *Journal of Geophysical Research: Atmospheres*, 121, 1859–1877, <https://doi.org/10.1002/2015JD023976>, 2016.

Kim, J., Cho, H.-K., Mok, J., Yoo, H. D., and Cho, N.: Effects of ozone and aerosol on surface UV radiation variability, *J Photochem Photobiol B*, 119, 46–51, <https://doi.org/10.1016/j.jphotobiol.2012.11.007>, 2013.

Kinne, S.: The MACv2 aerosol climatology, *Tellus B: Chemical and Physical Meteorology*, 71, 1–21, <https://doi.org/10.1080/16000889.2019.1623639>, 2019.

795 Kosmopoulos, P., Kouroutsidis, D., Papachristopoulou, K., Raptis, P. I., Masoom, A., Saint-Drenan, Y.-M., Blanc, P., Kontoes, C., and Kazadzis, S.: Short-Term Forecasting of Large-Scale Clouds Impact on Downwelling Surface Solar Irradiation, <https://doi.org/10.3390/en13246555>, 2020.

Kosmopoulos, P. G., Kazadzis, S., Schmalwieser, A. W., Raptis, P. I., Papachristopoulou, K., Fountoulakis, I., Masoom, A., Bais, A. F., Bilbao, J., Blumthaler, M., Kreuter, A., Siani, A. M., Eleftheratos, K., Topaloglou, C., Gröbner, J., Johnsen, B.,  
800 Svendby, T. M., Vilaplana, J. M., Doppler, L., Webb, A. R., Khazova, M., De Backer, H., Heikkilä, A., Lakkala, K., Jaroslawski, J., Meleti, C., Diémoz, H., Hülsen, G., Klotz, B., Rimmer, J., and Kontoes, C.: Real-time UV index retrieval in Europe using Earth observation-based techniques: system description and quality assessment, *Atmos. Meas. Tech.*, 14, 5657–5699, <https://doi.org/10.5194/amt-14-5657-2021>, 2021.

Krotkov, N. A., Bhartia, P. K., Herman, J. R., Fioletov, V., and Kerr, J.: Satellite estimation of spectral surface UV irradiance in the presence of tropospheric aerosols: 1. Cloud-free case, *Journal of Geophysical Research: Atmospheres*, 103, 8779–8793, <https://doi.org/10.1029/98JD00233>, 1998.

Krotkov, N. A., Herman, J. R., Bhartia, P. K., Fioletov, V., and Ahmad, Z.: Satellite estimation of spectral surface UV irradiance: 2. Effects of homogeneous clouds and snow, *Journal of Geophysical Research: Atmospheres*, 106, 11743–11759, <https://doi.org/10.1029/2000JD900721>, 2001.

810 Kylling, A., Albold, A., and Seckmeyer, G.: Transmittance of a cloud is wavelength-dependent in the UV-range: Physical interpretation, *Geophys Res Lett*, 24, 397–400, <https://doi.org/https://doi.org/10.1029/97GL00111>, 1997.

Lakkala, K., Arola, A., Heikkilä, A., Kaurola, J., Koskela, T., Kyrö, E., Lindfors, A., Meinander, O., Tanskanen, A., Gröbner, J., and Hülsen, G.: Quality assurance of the Brewer spectral UV measurements in Finland, *Atmos. Chem. Phys.*, 8, 3369–3383, <https://doi.org/10.5194/acp-8-3369-2008>, 2008.

815 Lakkala, K., Kujanpää, J., Brogniez, C., Henriot, N., Arola, A., Aun, M., Auriol, F., Bais, A. F., Bernhard, G., De Bock, V., Catalfamo, M., Deroo, C., Diémoz, H., Egli, L., Forestier, J.-B., Fountoulakis, I., Garane, K., Garcia, R. D., Gröbner, J., Hassinen, S., Heikkilä, A., Henderson, S., Hülsen, G., Johnsen, B., Kalakoski, N., Karanikolas, A., Karppinen, T., Lamy, K., León-Luis, S. F., Lindfors, A. V., Metzger, J.-M., Minvielle, F., Muskatel, H. B., Portafaix, T., Redondas, A., Sanchez, R., Siani, A. M., Svendby, T., and Tamminen, J.: Validation of the TROPOspheric Monitoring Instrument (TROPOMI) surface UV radiation product, *Atmos. Meas. Tech.*, 13, 6999–7024, <https://doi.org/10.5194/amt-13-6999-2020>, 2020.

Leveld, P. F., Hilsenrath, E., Leppelmeier, G. W., van den Oord, G. H. J., Bhartia, P. K., Tamminen, J., de Haan, J. F., and Veefkind, J. P.: Science objectives of the ozone monitoring instrument, *IEEE Transactions on Geoscience and Remote Sensing*, 44, 1199–1208, <https://doi.org/10.1109/TGRS.2006.872336>, 2006.

Lindfors, A. V., Kujanpää, J., Kalakoski, N., Heikkilä, A., Lakkala, K., Mielonen, T., Sneep, M., Krotkov, N. A., Arola, A.,  
825 and Tamminen, J.: The TROPOMI surface UV algorithm, *Atmos. Meas. Tech.*, 11, 997–1008, <https://doi.org/10.5194/amt-11-997-2018>, 2018.

Long, C. S., Miller, A. J., Lee, H.-T., Wild, J. D., Przywarty, R. C., and Hufford, D.: Ultraviolet Index Forecasts Issued by the National Weather Service, *Bull Am Meteorol Soc*, 77, 729–748, [https://doi.org/https://doi.org/10.1175/1520-0477\(1996\)077<0729:UFIGBT>2.0.CO;2](https://doi.org/https://doi.org/10.1175/1520-0477(1996)077<0729:UFIGBT>2.0.CO;2), 1996.

830 Lucas, R. M., Yazar, S., Young, A. R., Norval, M., de Gruyl, F. R., Takizawa, Y., Rhodes, L. E., Sinclair, C. A., and Neale, R. E.: Human health in relation to exposure to solar ultraviolet radiation under changing stratospheric ozone and climate, *Photochemical & Photobiological Sciences*, 18, 641–680, <https://doi.org/10.1039/C8PP90060D>, 2019.

Malinovic-Milicevic, S. and Mihailovic, D. T.: The use of NEOPLANTA model for evaluating the UV index in the Vojvodina region (Serbia), *Atmos Res*, 101, 621–630, <https://doi.org/10.1016/j.atmosres.2011.04.008>, 2011.

835 Mayer, B. and Kylling, A.: Technical note: The libRadtran software package for radiative transfer calculations - description and examples of use, *Atmos. Chem. Phys.*, 5, 1855–1877, <https://doi.org/10.5194/acp-5-1855-2005>, 2005.

Mayer, B., Seckmeyer, G., and Kylling, A.: Systematic long-term comparison of spectral UV measurements and UVSPEC modeling results, *Journal of Geophysical Research: Atmospheres*, 102, 8755–8767, <https://doi.org/10.1029/97JD00240>, 1997.

840 McKenzie, R., Bernhard, G., Liley, B., Disterhoft, P., Rhodes, S., Bais, A., Morgenstern, O., Newman, P., Oman, L., Brogniez, C., and Simic, S.: Success of Montreal Protocol Demonstrated by Comparing High-Quality UV Measurements with “World Avoided” Calculations from Two Chemistry-Climate Models, *Sci Rep*, 9, 12332, <https://doi.org/10.1038/s41598-019-48625-z>, 2019.

McKenzie, R. L. and Lucas, R. M.: Reassessing Impacts of Extended Daily Exposure to Low Level Solar UV Radiation, *Sci Rep*, 8, 13805, <https://doi.org/10.1038/s41598-018-32056-3>, 2018.

845 Météo-France: Algorithm Theoretical Basis Document for the Cloud Product Processors of the NWC/GEO (GEO-CMA-v4.0, GEO-CT-v3.0, GEO-CTTH-v3.0, GEO-CMIC-v1.0), Technical Report NWC/CDOP2/GEO/MFL/SCI/ATBD/Cloud, Issue 1, Rev. 1, Météo-France., 2016.

Mok, J., Krotkov, N. A., Arola, A., Torres, O., Jethva, H., Andrade, M., Labow, G., Eck, T. F., Li, Z., Dickerson, R. R., Stenchikov, G. L., Osipov, S., and Ren, X.: Impacts of brown carbon from biomass burning on surface UV and ozone 850 photochemistry in the Amazon Basin, *Sci Rep*, 6, 36940, <https://doi.org/10.1038/srep36940>, 2016.

Mok, J., Krotkov, N. A., Torres, O., Jethva, H., Li, Z., Kim, J., Koo, J.-H., Go, S., Irie, H., Labow, G., Eck, T. F., Holben, B. N., Herman, J., Loughman, R. P., Spinei, E., Lee, S. S., Khatri, P., and Campanelli, M.: Comparisons of spectral aerosol single scattering albedo in Seoul, South Korea, *Atmos Meas Tech*, 11, 2295–2311, <https://doi.org/10.5194/amt-11-2295-2018>, 2018.

Molina, L. T. and Molina, M. J.: Absolute absorption cross sections of ozone in the 185- to 350-nm wavelength range, *Journal 855 of Geophysical Research: Atmospheres*, 91, 14501–14508, <https://doi.org/10.1029/JD091iD13p14501>, 1986.

Morgenstern, O., Braesicke, P., Hurwitz, M. M., O’Connor, F. M., Bushell, A. C., Johnson, C. E., and Pyle, J. A.: The World Avoided by the Montreal Protocol, *Geophys Res Lett*, 35, <https://doi.org/https://doi.org/10.1029/2008GL034590>, 2008.

Newman, P. A. and McKenzie, R.: UV impacts avoided by the Montreal Protocol, *Photochemical & Photobiological Sciences*, 10, 1152–1160, <https://doi.org/10.1039/C0PP00387E>, 2011.

860 Papachristopoulou, K., Fountoulakis, I., Bais, A. F., Psiloglou, B. E., Papadimitriou, N., Raptis, I.-P., Kazantzidis, A., Kontoes, C., Hatzaki, M., and Kazadzis, S.: Effects of clouds and aerosols on downwelling surface solar irradiance nowcasting and short-term forecasting, *Atmos. Meas. Tech. Discuss.*, 2023, 1–31, <https://doi.org/10.5194/amt-2023-110>, 2023.

Papachristopoulou, K., Fountoulakis, I., Bais, A. F., Psiloglou, B. E., Papadimitriou, N., Raptis, I.-P., Kazantzidis, A., Kontoes, C., Hatzaki, M., and Kazadzis, S.: Effects of clouds and aerosols on downwelling surface solar irradiance nowcasting and short-term forecasting, *Atmos Meas Tech*, 17, 1851–1877, <https://doi.org/10.5194/amt-17-1851-2024>, 2024.

865 Parisi, A., Igoe, D., Downs, N., Turner, J., Amar, A., and A Jebar, M.: Satellite Monitoring of Environmental Solar Ultraviolet A (UVA) Exposure and Irradiance: A Review of OMI and GOME-2, *Remote Sens (Basel)*, 13, 752, <https://doi.org/10.3390/rs13040752>, 2021.

Peuch, V.-H., Engelen, R., Rixen, M., Dee, D., Flemming, J., Suttie, M., Ades, M., Agustí-Panareda, A., Ananasso, C., 870 Andersson, E., Armstrong, D., Barré, J., Bouserez, N., Dominguez, J. J., Garrigues, S., Inness, A., Jones, L., Kipling, Z., Letertre-Danczak, J., Parrington, M., Razinger, M., Ribas, R., Vermoote, S., Yang, X., Simmons, A., Garcés de Marcilla, J., and Thépaut, J.-N.: The Copernicus Atmosphere Monitoring Service: From Research to Operations, *Bull Am Meteorol Soc*, 103, E2650–E2668, [https://doi.org/https://doi.org/10.1175/BAMS-D-21-0314.1](https://doi.org/10.1175/BAMS-D-21-0314.1), 2022.

Pfeifer, M. T., Koepke, P., and Reuder, J.: Effects of altitude and aerosol on UV radiation, *Journal of Geophysical Research: 875 Atmospheres*, 111, <https://doi.org/10.1029/2005JD006444>, 2006.

Piacentini, R. D., Cede, A., and Bárcena, H.: Extreme solar total and UV irradiances due to cloud effect measured near the summer solstice at the high-altitude desertic plateau Puna of Atacama (Argentina), *J Atmos Sol Terr Phys*, 65, 727–731, [https://doi.org/10.1016/S1364-6826\(03\)00084-1](https://doi.org/10.1016/S1364-6826(03)00084-1), 2003.

Raptis, I.-P., Kazadzis, S., Eleftheratos, K., Amiridis, V., and Fountoulakis, I.: Single Scattering Albedo's Spectral Dependence 880 Effect on UV Irradiance, <https://doi.org/10.3390/atmos9090364>, 2018.

Redondas, A., Evans, R., Stuebi, R., Köhler, U., and Weber, M.: Evaluation of the use of five laboratory-determined ozone absorption cross sections in Brewer and Dobson retrieval algorithms, *Atmos Chem Phys*, 14, 1635–1648, <https://doi.org/10.5194/acp-14-1635-2014>, 2014.

Reuder, J. and Schwander, H.: Aerosol effects on UV radiation in nonurban regions, *Journal of Geophysical Research: 885 Atmospheres*, 104, 4065–4077, <https://doi.org/10.1029/1998JD200072>, 1999.

Rieder, H. E., Staehelin, J., Weihs, P., Vuilleumier, L., Maeder, J. A., Holawe, F., Blumthaler, M., Lindfors, A., Peter, T., Simic, S., Spichtinger, P., Wagner, J. E., Walker, D., and Ribatet, M.: Relationship between high daily erythemal UV doses, total ozone, surface albedo and cloudiness: An analysis of 30 years of data from Switzerland and Austria, *Atmos Res*, 98, 9–20, <https://doi.org/10.1016/j.atmosres.2010.03.006>, 2010.

890 Roshan, D. R., Koc, M., Abdallah, A., Martin-Pomares, L., Isaifan, R., and Fountoukis, C.: UV Index Forecasting under the Influence of Desert Dust: Evaluation against Surface and Satellite-Retrieved Data, <https://doi.org/10.3390/atmos11010096>, 2020.

Schenzinger, V., Kreuter, A., Klotz, B., Schwarzmann, M., and Gröbner, J.: On the production and validation of satellite based UV index maps, *Atmos. Meas. Tech. Discuss.*, 2023, 1–26, <https://doi.org/10.5194/amt-2023-188>, 2023.

895 Schmalwieser, A. W., Gröbner, J., Blumthaler, M., Klotz, B., De Backer, H., Bolsée, D., Werner, R., Tomsic, D., Metelka, L., Eriksen, P., Jepsen, N., Aun, M., Heikkilä, A., Duprat, T., Sandmann, H., Weiss, T., Bais, A., Toth, Z., Siani, A.-M., Vaccaro, L., Diémoz, H., Grifoni, D., Zipoli, G., Lorenzetto, G., Petkov, B. H., di Sarra, A. G., Massen, F., Yousif, C., Aculinin, A. A., den Outer, P., Svendby, T., Dahlback, A., Johnsen, B., Biszczuk-Jakubowska, J., Krzyscin, J., Henriques, D., Chubarova, N., Kolarž, P., Mijatovic, Z., Groselj, D., Pribulova, A., Gonzales, J. R. M., Bilbao, J., Guerrero, J. M. V., Serrano, A., Andersson, 900 S., Vuilleumier, L., Webb, A., and O'Hagan, J.: UV Index monitoring in Europe, *Photochemical & Photobiological Sciences*, 16, 1349–1370, <https://doi.org/10.1039/C7PP00178A>, 2017.

Schmucki, D. A. and Philipona, R.: UV radiation in the Alps: the altitude effect, 234–239, <https://doi.org/10.1111/12.452923>, 2002.

Schulz, M., Christophe, Y., Ramonet, M., Wagner, A., Eskes, H. J., Basart, S., Benedictow, A., Bennouna, Y., Blechschmidt, 905 A.-M., Chabrillat, S., Cuevas, E., El Yazidi, A., Flentje, H., Hansen, K. M., Im, U., Kapsomenakis, J., Langerock, B., Richter, A., Sudarchikova, N., Thouret, V., Warneke, T., and Zerefos, C.: Validation report of the CAMS near-real-time global atmospheric composition service: Period December 2018 -February 2019, *Copernicus Atmosphere Monitoring Service (CAMS) report, CAMS84\_2018SC1\_D1.1.1\_DJF2019\_v1.pdf*, June 2019, <https://doi.org/10.24380/7th6-tk72>, 2022.

Shettle, E.: Models of aerosols, clouds, and precipitation for atmospheric propagation studies, *AGARD Conf. Proce.*, 1, 1990.

910 Siani, A. M., Casale, G. R., Diémoz, H., Agnesod, G., Kimlin, M. G., Lang, C. A., and Colosimo, A.: Personal UV exposure in high albedo alpine sites, *Atmos Chem Phys*, 8, 3749–3760, <https://doi.org/10.5194/acp-8-3749-2008>, 2008.

Sola, Y., Lorente, J., Campmany, E., de Cabo, X., Bech, J., Redaño, A., Martínez-Lozano, J. A., Utrillas, M. P., Alados-Arboledas, L., Olmo, F. J., Díaz, J. P., Expósito, F. J., Cachorro, V., Sorribas, M., Labajo, A., Vilaplana, J. M., Silva, A. M., and Badosa, J.: Altitude effect in UV radiation during the Evaluation of the Effects of Elevation and Aerosols on the Ultraviolet 915 Radiation 2002 (VELETA-2002) field campaign, *Journal of Geophysical Research: Atmospheres*, 113, <https://doi.org/10.1029/2007JD009742>, 2008.

Staiger, H., den Outer, P. N., Bais, A. F., Feister, U., Johnsen, B., and Vuilleumier, L.: Hourly resolved cloud modification factors in the ultraviolet, *Atmos. Chem. Phys.*, 8, 2493–2508, <https://doi.org/10.5194/acp-8-2493-2008>, 2008.

Tanskanen, A., Krotkov, N. A., Herman, J. R., and Arola, A.: Surface ultraviolet irradiance from OMI, *IEEE Transactions on 920 Geoscience and Remote Sensing*, 44, 1267–1271, <https://doi.org/10.1109/TGRS.2005.862203>, 2006.

<https://www.temis.nl/uvradiation/UVArchive.php>: <https://www.temis.nl/uvradiation/UVArchive.php>.

Utrillas, M. P., Marín, M. J., Esteve, A. R., Salazar, G., Suárez, H., Castillo, J., and Martínez-Lozano, J. A.: UVER and UV index at high altitude in Northwestern Argentina, *J Photochem Photobiol B*, 163, 290–295, <https://doi.org/10.1016/j.jphotobiol.2016.08.012>, 2016.

925 Vanicek, K., Frei, T., Litynska, Z., and Schmalwieser, A.: UV-Index for the Public, *Publication of the European Communities*, Brussels, Belgium, 2000.

Verdebout, J.: A method to generate surface UV radiation maps over Europe using GOME, Meteosat, and ancillary geophysical data, *Journal of Geophysical Research: Atmospheres*, 105, 5049–5058, [https://doi.org/https://doi.org/10.1029/1999JD900302](https://doi.org/10.1029/1999JD900302), 2000.

930 Vitt, R., Laschewski, G., Bais, A., Diémoz, H., Fountoulakis, I., Siani, A.-M., and Matzarakis, A.: UV-Index Climatology for Europe Based on Satellite Data, *Atmosphere (Basel)*, 11, 727, <https://doi.org/10.3390/atmos11070727>, 2020.

Webb, A. R. and Engelsen, O.: Calculated Ultraviolet Exposure Levels for a Healthy Vitamin D Status, *Photochem Photobiol*, 82, 1697–1703, [https://doi.org/https://doi.org/10.1111/j.1751-1097.2006.tb09833.x](https://doi.org/10.1111/j.1751-1097.2006.tb09833.x), 2006.

Webb, A. R., Slaper, H., Koepke, P., and Schmalwieser, A. W.: Know Your Standard: Clarifying the CIE Erythema Action Spectrum, *Photochem Photobiol*, 87, 483–486, [https://doi.org/https://doi.org/10.1111/j.1751-1097.2010.00871.x](https://doi.org/10.1111/j.1751-1097.2010.00871.x), 2011.

935 Webb, A. R., Kazantzidis, A., Kift, R. C., Farrar, M. D., Wilkinson, J., and Rhodes, L. E.: Colour Counts: Sunlight and Skin Type as Drivers of Vitamin D Deficiency at UK Latitudes., *Nutrients*, 10, <https://doi.org/10.3390/nu10040457>, 2018.

Webb, A. R., Terenetskaya, I. P., Holick, M. F., van Dijk, A., McKenzie, R. L., Lucas, R. M., Young, A. R., Philipsen, P. A., and de Gruijl, F. R.: Previtamin D action spectrum: Challenging CIE towards a standard, *Lighting Research & Technology*, 940 14771535221122936, <https://doi.org/10.1177/14771535221122937>, 2022.

Weihs, P. and Webb, A. R.: Accuracy of spectral UV model calculations: 2. Comparison of UV calculations with measurements, *Journal of Geophysical Research: Atmospheres*, 102, 1551–1560, <https://doi.org/10.1029/96JD02621>, 1997.

945 Weihs, P., Lenoble, J., Blumthaler, M., Martin, T., Seckmeyer, G., Philipona, R., De la Casiniere, A., Sergent, C., Gröbner, J., Cabot, T., Masserot, D., Pichler, T., Pougatch, E., Rengarajan, G., Schmucki, D., and Simic, S.: Modeling the effect of an inhomogeneous surface albedo on incident UV radiation in mountainous terrain: Determination of an effective surface albedo, *Geophys Res Lett*, 28, 3111–3114, [https://doi.org/https://doi.org/10.1029/2001GL012986](https://doi.org/10.1029/2001GL012986), 2001.

WHO: Environmental Health Criteria 160 - Ultraviolet Radiation, 1994.

Zaratti, F., Forno, R. N., García Fuentes, J., and Andrade, M. F.: Erythemally weighted UV variations at two high-altitude locations, *Journal of Geophysical Research: Atmospheres*, 108, <https://doi.org/10.1029/2001JD000918>, 2003.

950 Zempila, M.-M., Koukouli, M.-E., Bais, A., Fountoulakis, I., Arola, A., Kouremeti, N., and Balis, D.: OMI/Aura UV product validation using NILU-UV ground-based measurements in Thessaloniki, Greece, *Atmos Environ*, 140, 283–297, <https://doi.org/https://doi.org/10.1016/j.atmosenv.2016.06.009>, 2016.

Zempila, M.-M., van Geffen, J. H. G. M., Taylor, M., Fountoulakis, I., Koukouli, M.-E., van Weele, M., van der A, R. J., Bais, A., Meleti, C., and Balis, D.: TEMIS UV product validation using NILU-UV ground-based measurements in Thessaloniki, 955 Greece, *Atmos. Chem. Phys.*, 17, 7157–7174, <https://doi.org/10.5194/acp-17-7157-2017>, 2017.

Zerefos, C., Fountoulakis, I., Eleftheratos, K., and Kazantzidis, A.: The long-term variability of human health related solar ultraviolet-B radiation doses for the 1980s to the end of 21st century, *Physiol Rev*, <https://doi.org/10.1152/physrev.00031.2022>, 2023.

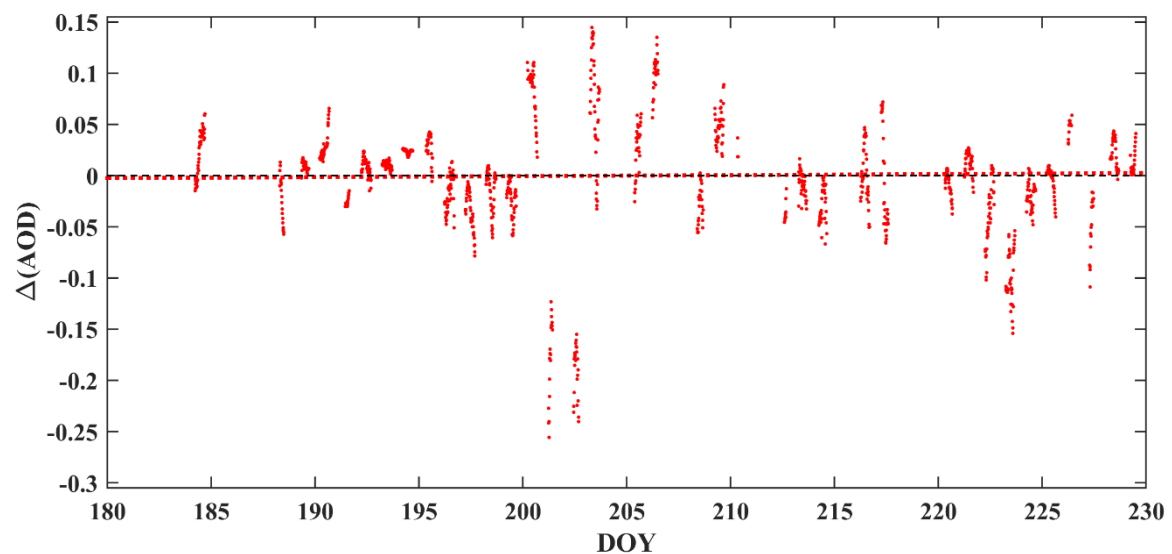
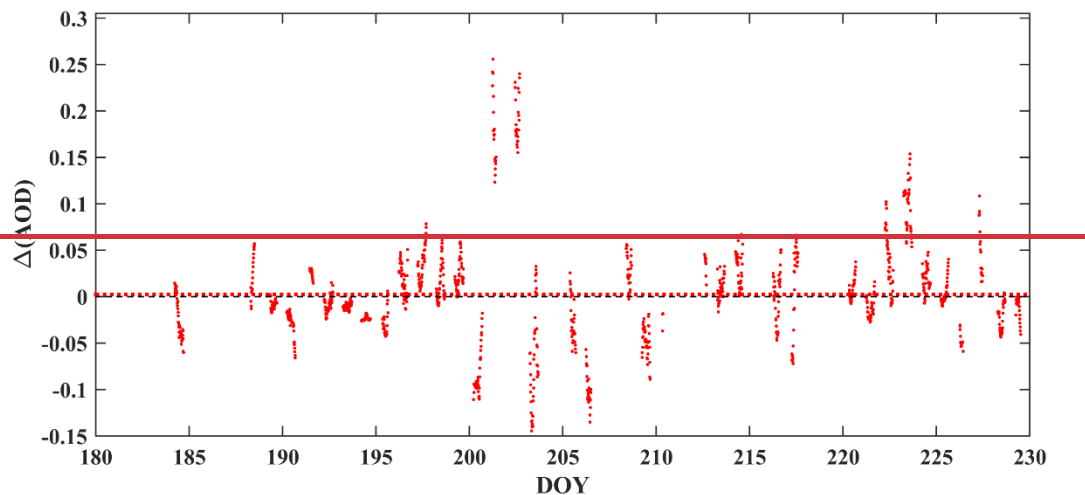


Figure A1: Differences between the 550 nm AOD from CAMS and the CIMEL (CAMS-CIMEL).

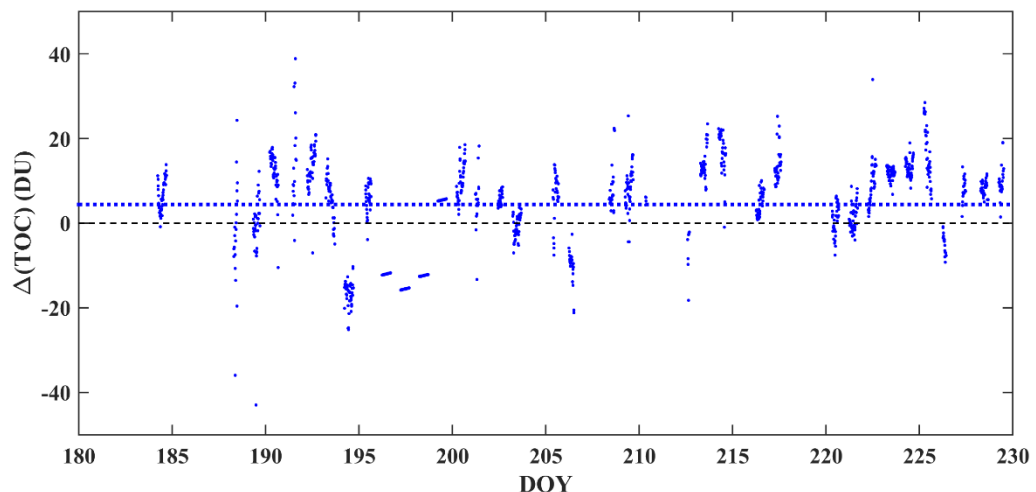


Figure A2: Differences between the TOC from TEMIS and the Brewer (TEMIS-Brewer).

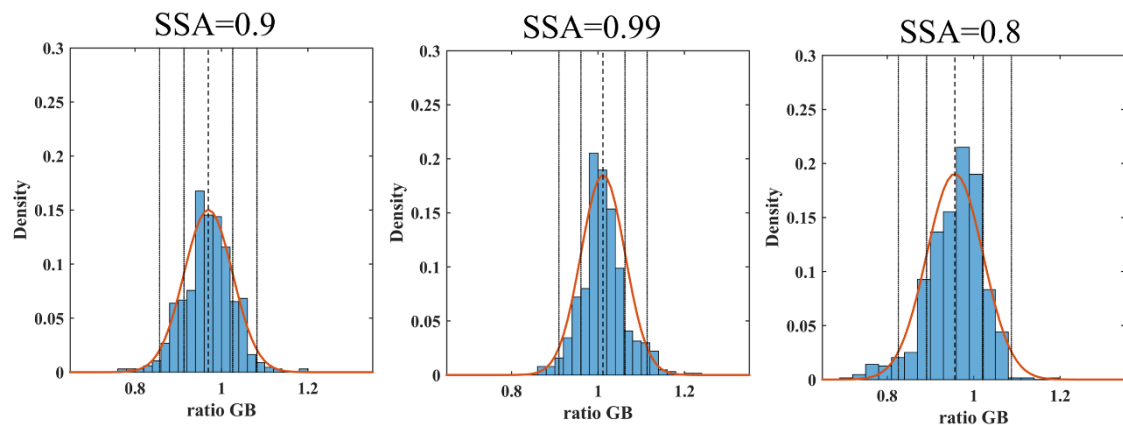


Figure A3: Density plots of the ratio between simulated (using GB measurements) and measured clear-sky UVI when different SSA values are used for the simulations. Vertical lines represent the mean and the 1-sigma and 2-sigma intervals if a normal distribution (red line) is assumed.